effects on gastric mucosal apoptosis and the inflammatory responses.

An ameliorative effect of HSP70 due to its cytoprotective, anti-inflammatory and molecular chaperone (quality control of proteins) properties has been reported for various diseases. For example, we have shown using transgenic mice expressing HSP70 that HSP70 protects against irritant-induced lesions in the stomach and small intestine, inflammatory bowel disease-related experimental colitis and UV-induced epidermal damage[7,8,30,42,43]. The potential therapeutic applicability of HSP70 for use in other diseases, such as neurodegenerative diseases, ischaemia–reperfusion damage and diabetes, has also been suggested[44–46]. Interestingly, geranylgeranylacetone, a leading anti-ulcer drug on the Japanese market, has been reported to be an HSP inducer, up-regulating various HSP not only in cultured gastric mucosal cells but also in various tissues *in vivo*[6]. It has been reported that geranylgeranylacetone suppresses not only gastric lesions but also lesions of the small intestine, inflammatory bowel disease-related experimental colitis and neurodegenerative diseases[8,42,47,48]. Therefore, the results of the present study suggest that LMW β-glucan may be beneficial not only for inhibiting the development of gastric lesions but also for the treatment of other diseases through the induction of HSP70 expression.

Acknowledgements

The present study was supported by Grants-in-Aid for Scientific Research from the Ministry of Health, Labour and Welfare of Japan, as well as the Japan Science and Technology Agency and Grants-in-Aid for Scientific Research from the Ministry of Education, Culture, Sports, Science and Technology, Japan. K.-i. T. and Y. T. did some of the experiments. T. S. prepared LMW β-glucan and T. M. is responsible for conducting the study. None of the authors has a financial relationship with a commercial entity that has an interest in the subject of the study.

References

1. Holzer P (1998) Neural emergency system in the stomach. *Gastroenterology* **114**, 823–839.
2. Miller TA (1983) Protective effects of prostaglandins against gastric mucosal damage: current knowledge and proposed mechanisms. *Am J Physiol* **245**, G601–G623.
3. Mathew A & Morimoto RI (1998) Role of the heat-shock response in the life and death of proteins. *Ann N Y Acad Sci* **851**, 99–111.
4. Gething MJ & Sambrook J (1992) Protein folding in the cell. *Nature* **355**, 33–45.
5. Kiang JG & Tsokos GC (1998) Heat shock protein 70 kDa: molecular biology, biochemistry, and physiology. *Pharmacol Ther* **80**, 183–201.
6. Hirakawa T, Rokutan K, Nikawa T, *et al.* (1996) Geranylgeranylacetone induces heat shock proteins in cultured guinea pig gastric mucosal cells and rat gastric mucosa. *Gastroenterology* **111**, 345–357.
7. Tanaka K, Tsutsumi S, Arai Y, *et al.* (2007) Genetic evidence for a protective role of heat shock factor 1 against irritant-induced gastric lesions. *Mol Pharmacol* **71**, 985–993.
8. Suemasu S, Tanaka K, Namba T, *et al.* (2009) A role for HSP70 in protecting against indomethacin-induced gastric lesions. *J Biol Chem* **284**, 19705–19715.
9. Tsoni SV & Brown GD (2008) beta-Glucans and dectin-1. *Ann N Y Acad Sci* **1143**, 45–60.
10. Chen J & Seviour R (2007) Medicinal importance of fungal beta-(1 → 3), (1 → 6)-glucans. *Mycol Res* **111**, 635–652.
11. Brown GD & Gordon S (2003) Fungal beta-glucans and mammalian immunity. *Immunity* **19**, 311–315.
12. Hashimoto T, Ohno N, Adachi Y, *et al.* (1997) Enhanced production of inducible nitric oxide synthase by beta-glucans in mice. *FEMS Immunol Med Microbiol* **19**, 131–135.
13. Engstad CS, Engstad RE, Olsen JO, *et al.* (2002) The effect of soluble beta-1,3-glucan and lipopolysaccharide on cytokine production and coagulation activation in whole blood. *Int Immunopharmacol* **2**, 1585–1597.
14. Kimura Y, Sumiyoshi M, Suzuki T, *et al.* (2006) Antitumor and antimetastatic activity of a novel water-soluble low molecular weight beta-1, 3-D-glucan (branch beta-1,6) isolated from *Aureobasidium pullulans* 1A1 strain black yeast. *Anticancer Res* **26**, 4131–4141.
15. Berdal M, Appelbom HI, Eikrem JH, *et al.* (2007) Aminated beta-1,3-D-glucan improves wound healing in diabetic db/db mice. *Wound Repair Regen* **15**, 825–832.
16. Bell S, Goldman VM, Bistrian BR, *et al.* (1999) Effect of beta-glucan from oats and yeast on serum lipids. *Crit Rev Food Sci Nutr* **39**, 189–202.
17. Sener G, Eksioglu-Demiralp E, Cetiner M, *et al.* (2006) Beta-glucan ameliorates methotrexate-induced oxidative organ injury via its antioxidant and immunomodulatory effects. *Eur J Pharmacol* **542**, 170–178.
18. Bedirli A, Kerem M, Pasaoglu H, *et al.* (2007) Beta-glucan attenuates inflammatory cytokine release and prevents acute lung injury in an experimental model of sepsis. *Shock* **27**, 397–401.
19. Lyuksutova OI, Murphey ED, Toliver-Kinsky TE, *et al.* (2005) Glucan phosphate treatment attenuates burn-induced inflammation and improves resistance to *Pseudomonas aeruginosa* burn wound infection. *Shock* **23**, 224–232.
20. Soltys J & Quinn MT (1999) Modulation of endotoxin- and enterotoxin-induced cytokine release by *in vivo* treatment with beta-(1,6)-branched beta-(1,3)-glucan. *Infect Immun* **67**, 244–252.
21. Toklu HZ, Sehirli AO, Velioglu-Ogunc A, *et al.* (2006) Acetaminophen-induced toxicity is prevented by beta-D-glucan treatment in mice. *Eur J Pharmacol* **543**, 133–140.
22. Shah VB, Williams DL & Keshvara L (2009) beta-Glucan attenuates TLR2- and TLR4-mediated cytokine production by microglia. *Neurosci Lett* **458**, 111–115.
23. Sumiyoshi M, Suzuki T & Kimura Y (2009) Protective effects of water-soluble low-molecular-weight beta-(1,3–1,6)D-glucan purified from *Aureobasidium pullulans* GM-NH-1A1 against UFT toxicity in mice. *J Pharm Pharmacol* **61**, 795–800.
24. Ha T, Hua F, Grant D, *et al.* (2006) Glucan phosphate attenuates cardiac dysfunction and inhibits cardiac MIF expression and apoptosis in septic mice. *Am J Physiol Heart Circ Physiol* **291**, H1910–H1918.
25. Kimura Y, Sumiyoshi M, Suzuki T, *et al.* (2007) Effects of water-soluble low-molecular-weight beta-1,3-D-glucan (branch beta-1,6) isolated from *Aureobasidium pullulans* 1A1 strain black yeast on restraint stress in mice. *J Pharm Pharmacol* **59**, 1137–1144.

BJN British Journal of Nutrition

26. Kimura Y, Sumiyoshi M, Suzuki T, *et al.* (2007) Inhibitory effects of water-soluble low-molecular-weight beta-(1,3–1,6) D-glucan purified from *Aureobasidium pullulans* GM-NH-1A1 strain on food allergic reactions in mice. *Int Immunopharmacol* **7**, 963–972.
27. Futaki N, Arai I, Hamasaka Y, *et al.* (1993) Selective inhibition of NS-398 on prostanoid production in inflamed tissue in rat carrageenan-air-pouch inflammation. *J Pharm Pharmacol* **45**, 753–755.
28. Mima S, Tsutsumi S, Ushijima H, *et al.* (2005) Induction of claudin-4 by nonsteroidal anti-inflammatory drugs and its contribution to their chemopreventive effect. *Cancer Res* **65**, 1868–1876.
29. Krawisz JE, Sharon P & Stenson WF (1984) Quantitative assay for acute intestinal inflammation based on myeloperoxidase activity. Assessment of inflammation in rat and hamster models. *Gastroenterology* **87**, 1344–1350.
30. Tanaka K, Namba T, Arai Y, *et al.* (2007) Genetic evidence for a protective role for heat shock factor 1 and heat shock protein 70 against colitis. *J Biol Chem* **282**, 23240–23252.
31. Bradford MM (1976) A rapid and sensitive method for the quantitation of microgram quantities of protein utilizing the principle of protein–dye binding. *Anal Biochem* **72**, 248–254.
32. Salimuddin, Nagasaki A, Gotoh T, *et al.* (1999) Regulation of the genes for arginase isoforms and related enzymes in mouse macrophages by lipopolysaccharide. *Am J Physiol* **277**, E110–E117.
33. Nagasaki A, Gotoh T, Takeya M, *et al.* (1996) Coinduction of nitric oxide synthase, argininosuccinate synthetase, and argininosuccinate lyase in lipopolysaccharide-treated rats. RNA blot, immunoblot, and immunohistochemical analyses. *J Biol Chem* **271**, 2658–2662.
34. Tsutsumi S, Tomisato W, Takano T, *et al.* (2002) Gastric irritant-induced apoptosis in guinea pig gastric mucosal cells in primary culture. *Biochim Biophys Acta* **1589**, 168–180.
35. Corfield AP, Myerscough N, Longman R, *et al.* (2000) Mucins and mucosal protection in the gastrointestinal tract: new prospects for mucins in the pathology of gastrointestinal disease. *Gut* **47**, 589–594.
36. Byrd JC & Bresalier RS (2004) Mucins and mucin binding proteins in colorectal cancer. *Cancer Metastasis Rev* **23**, 77–99.
37. Kim HP, Wang X, Zhang J, *et al.* (2005) Heat shock protein-70 mediates the cytoprotective effect of carbon monoxide: involvement of p38 beta MAPK and heat shock factor-1. *J Immunol* **175**, 2622–2629.
38. Wang X, Khaleque MA, Zhao MJ, *et al.* (2006) Phosphorylation of HSF1 by MAPK-activated protein kinase 2 on serine 121, inhibits transcriptional activity and promotes HSP90 binding. *J Biol Chem* **281**, 782–791.
39. Rice PJ, Adams EL, Ozment-Skelton T, *et al.* (2005) Oral delivery and gastrointestinal absorption of soluble glucans stimulate increased resistance to infectious challenge. *J Pharmacol Exp Ther* **314**, 1079–1086.
40. Chen H, Wu Y, Zhang Y, *et al.* (2006) Hsp70 inhibits lipopolysaccharide-induced NF-kappaB activation by interacting with TRAF6 and inhibiting its ubiquitination. *FEBS Lett* **580**, 3145–3152.
41. Weiss YG, Bromberg Z, Raj N, *et al.* (2007) Enhanced heat shock protein 70 expression alters proteasomal degradation of IkappaB kinase in experimental acute respiratory distress syndrome. *Crit Care Med* **35**, 2128–2138.
42. Asano T, Tanaka K, Yamakawa N, *et al.* (2009) HSP70 confers protection against indomethacin-induced lesions of the small intestine. *J Pharmacol Exp Ther* **330**, 458–467.
43. Matsuda M, Hoshino T, Yamashita Y, *et al.* (2010) Prevention of UVB radiation-induced epidermal damage by expression of heat shock protein 70. *J Biol Chem* **285**, 5848–5858.
44. Jana NR, Tanaka M, Wang G, *et al.* (2000) Polyglutamine length-dependent interaction of Hsp40 and Hsp70 family chaperones with truncated N-terminal huntingtin: their role in suppression of aggregation and cellular toxicity. *Hum Mol Genet* **9**, 2009–2018.
45. Morimoto RI & Santoro MG (1998) Stress-inducible responses and heat shock proteins: new pharmacologic targets for cytoprotection. *Nat Biotechnol* **16**, 833–838.
46. Adachi H, Katsuno M, Minamiyama M, *et al.* (2003) Heat shock protein 70 chaperone overexpression ameliorates phenotypes of the spinal and bulbar muscular atrophy transgenic mouse model by reducing nuclear-localized mutant androgen receptor protein. *J Neurosci* **23**, 2203–2211.
47. Ohkawara T, Nishihira J, Takeda H, *et al.* (2005) Geranylgeranylacetone protects mice from dextran sulfate sodium-induced colitis. *Scand J Gastroenterol* **40**, 1049–1057.
48. Katsuno M, Sang C, Adachi H, *et al.* (2005) Pharmacological induction of heat-shock proteins alleviates polyglutamine-mediated motor neuron disease. *Proc Natl Acad Sci U S A* **102**, 16801–16806.

British Journal of Nutrition

Neurobiology of Disease

Suppression of Alzheimer's Disease-Related Phenotypes by Expression of Heat Shock Protein 70 in Mice

Tatsuya Hoshino,[1] Naoya Murao,[1] Takushi Namba,[1] Masaya Takehara,[1] Hiroaki Adachi,[2] Masahisa Katsuno,[2] Gen Sobue,[2] Takahide Matsushima,[3] Toshiharu Suzuki,[3] and Tohru Mizushima[1]

[1]Graduate School of Medical and Pharmaceutical Sciences, Kumamoto University, Kumamoto 862-0973, Japan, [2]Nagoya University Graduate School of Medicine, Nagoya 466-8550, Japan, and [3]Graduate School of Pharmaceutical Sciences, Hokkaido University, Sapporo 060-0812, Japan

Amyloid-β peptide (Aβ) plays an important role in the pathogenesis of Alzheimer's disease (AD). Aβ is generated by proteolysis of β-amyloid precursor protein (APP) and is cleared by enzyme-mediated degradation and phagocytosis by microglia and astrocytes. Some cytokines, such as TGF-β1, stimulate this phagocytosis. In contrast, cellular upregulation of HSP70 expression provides cytoprotection against Aβ. HSP70 activity in relation to inhibition of Aβ oligomerization and stimulation of Aβ phagocytosis has also been reported. Although these *in vitro* results suggest that stimulating the expression of HSP70 could prove effective in the treatment of AD, there is a lack of *in vivo* evidence supporting this notion. In this study, we address this issue, using transgenic mice expressing HSP70 and/or a mutant form of APP (APPsw). Transgenic mice expressing APPsw showed less of an apparent cognitive deficit when they were crossed with transgenic mice expressing HSP70. Transgenic mice expressing HSP70 also displayed lower levels of Aβ, Aβ plaque deposition, and neuronal and synaptic loss than control mice. Immunoblotting experiments and direct measurement of β- and γ-secretase activity suggested that overexpression of HSP70 does not affect the production Aβ. In contrast, HSP70 overexpression did lead to upregulation of the expression of Aβ-degrading enzyme and TGF-β1 both *in vivo* and *in vitro*. These results suggest that overexpression of HSP70 in mice suppresses not only the pathological but also the functional phenotypes of AD. This study provides the first *in vivo* evidence confirming the potential therapeutic benefit of HSP70 for the prevention or treatment of AD.

Introduction

Alzheimer's disease (AD) is characterized pathologically by the accumulation of neurofibrillary tangles and senile plaques, the latter of which are composed of amyloid-β peptide (Aβ), such as Aβ40 and Aβ42 (Hardy and Selkoe, 2002; Mattson, 2004). To generate Aβ, β-amyloid precursor protein (APP) is first cleaved by β-secretase and then by γ-secretase (Hardy and Selkoe, 2002; Mattson, 2004). Aβ can be cleared from the brain via three main pathways: degradation by enzymes, such as neprilysin, insulin-degrading enzyme (IDE), and endothelin-converting enzyme 2 (ECE-2), phagocytosis by microglia and astrocytes, and transport into the blood and lymph nodes (Miners et al., 2008; Zlokovic, 2008; Rodríguez et al., 2009). However, monomeric Aβ easily self-assembles to form oligomers, protofibrils, and fibrils, and it is now believed that less aggregated forms of Aβ, such as oligomers and protofibrils, are more important than the highly aggregated forms (Haass and Selkoe, 2007). Therefore, cellular factors that affect the production and clearance of Aβ and/or oligomerization of Aβ may be good targets for the development of drugs to prevent or treat AD.

When cells are exposed to stressors, heat shock proteins (HSPs) are induced, and the cellular upregulation of their expression, especially that of HSP70, provides resistance as the HSPs refold or degrade denatured proteins produced by the stressors (Morimoto and Santoro, 1998; Muchowski and Wacker, 2005). Not only AD but also other neurodegenerative diseases display aggregation of proteins, and overexpression of HSP70 (polyglutamine diseases) or HSP104 (Parkinson's disease) in animal models suppresses the aggregation of each pathogenic protein and ameliorates the corresponding disease symptoms (Adachi et al., 2003; Katsuno et al., 2005; Muchowski and Wacker, 2005; Lo Bianco et al., 2008). An increased level of expression of HSPs, such as small HSPs and HSP70 in the brain of AD patients, has been reported in a number of studies (Perez et al., 1991; Muchowski and Wacker, 2005), with *in vitro* experiments suggesting that expression of HSPs, in particular HSP70, could suppress the progression of AD (Magrané et al., 2004; Muchowski and Wacker, 2005; Evans et al., 2006; Kumar et al., 2007; Yoshiike et al., 2008). In terms of *in vivo* studies, the effect of overexpression of HSPs on the pathogenesis of AD has not been examined in vertebrate models. In this study, we investigated the effect of overexpression of HSP70 on AD-related phenotypes, using transgenic mice expressing HSP70 and/or a mutant (Swedish) type of APP (APPsw). Our results demonstrate that overexpression of HSP70 suppresses not only the pathological phenotypes of AD

Received Oct. 19, 2010; revised Jan. 11, 2011; accepted Jan. 14, 2011.

This work was supported by Grants-in-Aid for Scientific Research from the Ministry of Health, Labour, and Welfare of Japan, as well as the Japan Science and Technology Agency, Grants-in-Aid for Scientific Research from the Ministry of Education, Culture, Sports, Science and Technology, Japan. We thank Drs. M. Staufenbiel (Novartis Institutes for BioMedical Research, Basel, Switzerland), and C. E. Angelidis and G. N. Pagoulatos (University of Ioannina, Ioannina, Greece) for providing transgenic mice.

Correspondence should be addressed to Tohru Mizushima, Graduate School of Medical and Pharmaceutical Sciences, Kumamoto University, 5-1 Oe-honmachi, Kumamoto 862-0973, Japan. E-mail: mizu@gpo.kumamoto-u.ac.jp.

DOI:10.1523/JNEUROSCI.5478-10.2011

 0270-6474/11/315225-10$15.00/0

but also the resultant cognitive deficits, possibly through its effects on antiaggregation, neuroprotection, and stimulation of Aβ clearance.

Materials and Methods

Materials. Eagle's minimal essential medium (EMEM) was obtained from Nissui Pharmaceutical. A fluorescent substrate for β-secretase [H_2N-Arg-Glu-(EDANS)-Glu-Val-Asn-Leu-Asp-Ala-Glu-Phe-Lys-(DABCYL)-Arg-O] was purchased from Calbiochem and that for γ-secretase [Nma-Gly-Gly-Val-Val-Ile-Ala-Thr-Val-Lys(Dnp)-D-Arg-D-Arg-D-Arg-NH_2] and synthetic Aβ were obtained from Peptide Institute. Alexa Fluor 488 goat anti-mouse IgG, Neurobasal medium, B27, and an antibody to Aβ oligomer (A11) were purchased from Invitrogen. Sandwich ELISA (sELISA) kit for Aβ oligomers was obtained from Immunobiological Laboratories. An antibody to actin was obtained from Santa Cruz. Fetal bovine serum (FBS), thioflavin-S, and antibodies to the C-terminal fragment (CTF) of APP and synaptophysin were purchased from Sigma-Aldrich. An antibody to Aβ (6E10) came from Covance Research Products. An antibody to HSP70 was from Assay Designs, and those against neuronal nuclei (NeuN) and presenilin 1 (PS1) were from Millipore Bioscience Research Reagents. The RNeasy kit was obtained from QIAGEN. PrimeScript first-strand cDNA Synthesis kit was from Takara Bio, and iQ SYBR Green Supermix was purchased from Bio-Rad. ELISA kits for tumor necrosis factor-α (TNF-α), interleukin-1β (IL-1β), and IL-6 were from Pierce. An ELISA kit for TGF-β1 was obtained from R&D Systems. Sandwich ELISA kits for Aβ40 and Aβ42 and ara-C (cytarabine) were from Wako. Mounting medium for immunohistochemical analysis (VECTASHIELD) was from Vector Laboratories. Mayer's hematoxylin and mounting medium for histological examination (malinol) were purchased from Muto Pure Chemicals. The Envision kit was from Dako.

Animals. Transgenic mice that express APPsw (APP23, C57BL/6) were a gift from Dr. M. Staufenbiel (Novartis Institutes for BioMedical Research, Basel, Switzerland) (Sturchler-Pierrat et al., 1997). Transgenic mice expressing HSP70 were gifts from Drs. C. E. Angelidis and G. N. Pagoulatos (University of Ioannina, Ioannina, Greece) and crossed with C57BL/6 wild-type mice (WT/WT) 10 times to generate WT/HSP70 mice (Tanaka et al., 2007). APP23 male mice were crossed with WT/HSP70 female mice to generate APPsw/HSP70 mice. Parallel crosses were made between APP23 mice and WT/WT mice to generate APPsw/WT animals. All experiments in this study were done using female mice.

The experiments and procedures described here were performed in accordance with the *Guide for the Care and Use of Laboratory Animals* as adopted and promulgated by the National Institutes of Health and were approved by the Animal Care Committee of Kumamoto University.

Morris water maze test. The Morris water maze test was conducted in a circular 90-cm-diameter pool filled with water at a temperature of 22.0 ± 1°C, as described previously (Kobayashi et al., 2000; Huang et al., 2006), with minor modifications. In the hidden platform test, a circular platform (10 cm in diameter) was submerged 0.5 cm below water level. Swimming paths were tracked for 60 s with a camera and stored in a computer (Video Tracking System CompACT VAS/DV; Muromachi kikai). The mice were given four trials (one block) per day for 7 consecutive days, during which the platform was left in the same position. The time taken to reach the platform (escape latency) was measured, and the average of four trials was determined.

Twenty-four hours after the last trial of the hidden platform test, the mice were subjected to a transfer test in which the platform was removed, and their swimming path was recorded for 60 s. Percentage search time for each quadrant and crossing time in the area where the platform had been located were determined.

sELISA for Aβ or Aβ oligomer and ELISA for cytokines. Cells were cultured for 48 h, and the conditioned medium was subjected to sELISA for Aβ, as described previously (Tomita et al., 1998b; Hoshino et al., 2007a).

Aβ40, Aβ42, and cytokine levels in the brain were determined as described previously (Iwata et al., 2004). Briefly, the brain hemispheres were homogenized in 50 mM Tris/HCl buffer, pH 7.6, containing 150 mM NaCl, and then centrifuged. Guanidine/HCl (0.5 M, final concentration) was added to the supernatants (soluble fractions). The precipitates were solubilized by sonication in 6 M guanidine/HCl, after which the solubilized pellet was centrifuged and the resulting supernatant diluted (insoluble fractions). The amount of Aβ40 and Aβ42 in each fraction was determined by sELISA. An ELISA assay for Aβ oligomers or cytokines was performed on the soluble fractions (but without guanidine/HCl), according to the manufacturer's instructions.

Thioflavin-S staining and immunohistochemical analyses. The brain hemispheres were fixed in 4% buffered paraformaldehyde and embedded in paraffin before being cut into 4-μm-thick sections, which were then deparaffinized and washed in PBS.

For thioflavin-S staining, sections were stained with 1% thioflavin-S solution. Samples were mounted with malinol and inspected using a BX51 microscope (Olympus). Fluorescence microscopic images at region (1.0 mm^2) in the hippocampus and cerebral cortex were used to calculate the area stained with thioflavin-S using the LuminaVision (Mitani). By determining the threshold optical density, we divided into thioflavin-S-positive and -negative area and the percentage of thioflavin-S-positive area to total area was determined. We prepared three sections per mouse and calculated the average of values in three sections.

For immunohistochemical analysis to detect NeuN and HSP70, sections were incubated with 0.3% hydrogen peroxide in methanol for removal of endogenous peroxidase. They were then blocked with 2.5% goat serum for 10 min, and incubated for 12 h with antibody to NeuN (1:1000 dilution) or HSP70 (1:100 dilution) in the presence of 2.5% bovine serum albumin (BSA), followed by incubation for 1 h with peroxidase-labeled polymer conjugated to goat anti-mouse (for NeuN) or anti-rabbit (for HSP70) Ig. 3,3′-Diaminobenzidine was applied to the sections, which were then incubated with Mayer's hematoxylin. Samples were mounted with malinol and inspected using a BX51 microscope. NeuN-positive cells in the pyramidal cell layer of the hippocampal CA3 region (within 500 μm from the edge of the dentate gyrus) were counted. We prepared three sections per mouse and calculated the average of values in three sections.

For immunohistochemical analysis to detect synaptophysin, sections were blocked with 2.5% goat serum (v/v) for 10 min, incubated for 12 h with antibody to synaptophysin (1:200 dilution) in the presence of 2.5% BSA, and then incubated with Alexa Fluor 488 goat anti-mouse IgG. Samples were mounted with VECTASHIELD and inspected with the aid of a BX51 fluorescence microscope. Fluorescence intensity in area (100 × 150 μm) of the hippocampal CA3 region was determined using LuminaVision and shown relative to fluorescence intensity in wild-type mice. We prepared three sections per mouse and calculated the average of values in three sections.

Immunoblotting analysis. Whole-cell extracts were prepared as described previously (Hoshino et al., 2003). The protein concentration of each sample was determined by the Bradford method (Bradford, 1976). Samples were applied to SDS polyacrylamide gels (Tris/tricine gel for detection of Aβ, CTFα, and CTFβ or Tris/glycine gel for detection of other proteins) and subjected to electrophoresis, after which proteins were immunoblotted with each antibody.

A dot blotting assay for Aβ oligomer was performed on the soluble fractions (but without guanidine/HCl), as described previously (Wang et al., 2007). Proteins (4 μg) of soluble fractions were applied to nitrocellulose membrane, after which proteins were detected with antibody against Aβ oligomer (A11).

β- and γ-secretase-mediated peptide cleavage assay. β- and γ-secretase activity was monitored as previously reported (Fukumoto et al., 2002; Farmery et al., 2003). Solubilized membranes were incubated for 1 h at 37°C in 200 μl of 50 mM acetate buffer, pH 4.1, containing 100 mM sodium chloride, 0.025% BSA, and 10 μM β-secretase fluorescent substrate or for 4 h at 37°C in 200 μl of 50 mM Tris/HCl buffer, pH 6.8, containing 2 mM EDTA, 0.25% CHAPSO (3-[(3-cholamidopropyl)dimethylammonio]-2-hydroxy-1-propanesulfonate), and 10 μM γ-secretase fluorescent substrate. Fluorescence was measured using a plate reader (Fluostar Galaxy; BMG Labtech) with an excitation wavelength of 355 nm and an emission wavelength of 510 nm (for β-secretase) or 440 nm (for γ-secretase).

Real-time reverse transcription-PCR analysis. Real-time reverse transcription (RT)-PCR was performed as previously described (Mima et al., 2005) with some modifications. Total RNA was extracted from the brain

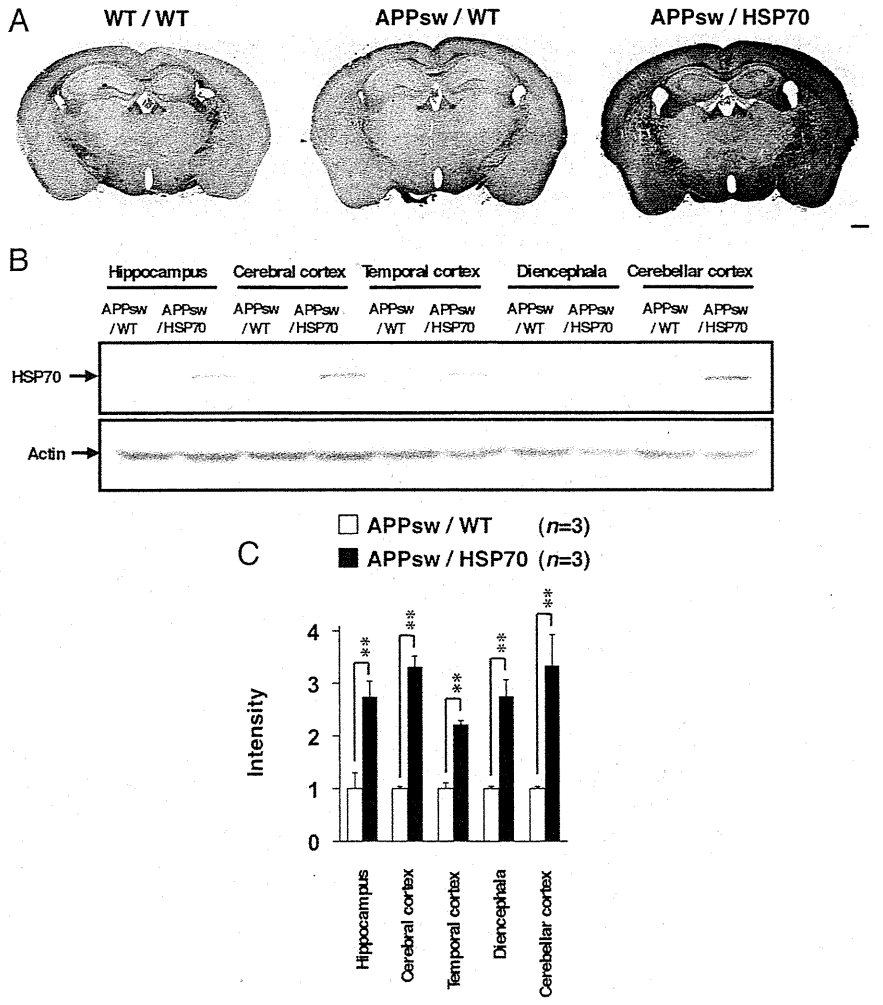

Figure 1. Expression of HSP70 in the brain. ***A***, ***B***, Brains were removed from WT/WT, APPsw/WT, and APPsw/HSP70 mice at the age of 18 months. ***A***, Sections were prepared and subjected to immunohistochemical analysis with an antibody to HSP70. Scale bar, 500 μm. ***B***, Brains were divided into fractions containing the hippocampus, cerebral cortex, temporal cortex, diencephala, and cerebellar cortex. Whole-cell extracts were then prepared from each fraction and subjected to immunoblotting with an antibody to HSP70 or actin. ***C***, The band intensity of HSP70 was determined, corrected with that of actin, and expressed relative to the control ($n = 3$). $^{**}p < 0.01$. Error bars indicate SEM.

or cultured cells using an RNeasy kit according to the manufacturer's protocol. Samples (1 μg of RNA) were reverse-transcribed using a first-strand cDNA synthesis kit. Synthesized cDNA was used in real-time RT-PCR (Chromo 4 instrument; Bio-Rad) experiments using iQ SYBR GREEN Supermix, and then analyzed with Opticon Monitor Software. Specificity was confirmed by electrophoretic analysis of the reaction products and by inclusion of template- or reverse transcriptase-free controls. To normalize the amount of total RNA present in each reaction, glyceraldehyde-3-phosphate dehydrogenase (GAPDH) cDNA was used as an internal standard.

Primers were designed using the Primer3 website. The primers used were as follows (name: forward primer, reverse primer): *gapdh*: 5′-aactttggcatt-gtggaagg-3′, 5′-acacattgggggtaggaaca-3′; *neprilysin*: 5′-gcagcctcagccgaaac-tac-3′, 5′-caccgtctccatgttgcagt-3′; *ide*: 5′-accaggaaatgttggctgtc-3′, 5′-tct-gagaggggaactctcca-3′; *ece-2*: 5′-gctatgcccatgtacccagt-3′, 5′-tggcatccagagtac-ccttc-3′; *il-1β*: 5′-gatcccaagcaatacccaaa-3′, 5′-ggggaactctgcagactcaa-3′; *il-6*: 5′-ctggagtcacagaaggagtgg-3′, 5′-ggtttgccgagtagatctcaa-3′; *tnf-α*: 5′-cgtcagc-cgatttgctatct-3′, 5′-cggactccgcaaagtctaag-3′; *tgf-β1*: 5′-tgacgtcactggagtacgg-3′, 5′-ggttcatgtcatggatggtgc-3′.

Cell culture. The primary culture of cortical neurons was done as described previously (Saito et al., 2008). The cortex of embryonic day 15.5 mice was dissected. Neurons were spread in a buffer containing papain and cultured at 5×10^4 cells cm^{-2} in Neurobasal medium containing B27 and antibiotics on poly-D-lysine-coated dishes.

Primary cultures of microglia and astrocytes were prepared as described previously (Kauppinen and Swanson, 2005). The cortex of 1-d-old mice was dissected. Cells were spread in a buffer containing papain and DNase and cultured at 1×10^6 cells cm^{-2} in EMEM containing 10 mM HEPES/KOH and 10% FBS for 2 weeks. Microglial cells were obtained by mildly shaking and collecting the floating cells. For preparation of astrocytes, cells were further incubated in EMEM containing 10 mM HEPES/KOH, 10% FBS, and 20 μM ara-C for 3 d to induce microglial cell death.

Statistical analysis. All values are expressed as the mean ± SEM or SD. Two-way ANOVA followed by Tukey's test was used to evaluate differences between more than three groups. Student's *t* test for unpaired results was used for the evaluation of differences between two groups. Differences were considered to be significant for values of $p < 0.05$.

Results

Effect of overexpression of HSP70 on cognitive function in transgenic mice expressing APPsw

To examine the effect of overexpression of HSP70 on the pathogenesis of AD, we used transgenic mice expressing APPsw (APP23, AD model mice) crossed to transgenic mice that express human HSP70 under the control of the human β-actin promoter (Plumier et al., 1995). The overexpression of HSP70 in the mice has been demonstrated in various organs, including the brain (Plumier et al., 1997). We first confirmed the expression of HSP70 in the brain by immunohistochemical analysis. As shown in Figure 1*A*, a higher level of HSP70 expression was observed in various brain regions, including the hippocampus and cerebral cortex, in the HSP70 transgenic mice (APPsw/HSP70) at the age of 18 months when compared with the control animals (WT/WT and APPsw/WT). We also compared the level of HSP70 in various parts of the brain by immunoblotting. Higher levels of HSP70 were observed in all regions of the brain tested (hippocampus, cerebral cortex, temporal cortex, diencephala, and cerebellar cortex) in the APPsw/HSP70 mice at the age of 18 months than in the APPsw/WT mice (Fig. 1*B*). Similar results were observed APPsw/HSP70 mice at the age of 12 months (supplemental Fig. 1, available at www.jneurosci.org as supplemental material).

We then used a Morris water maze to examine the effect of overexpression of HSP70 on spatial learning and memory. Four strains of mice (WT/WT, WT/HSP70, APPsw/WT, and APPsw/HSP70) were trained to learn the location of a hidden platform four times per day for 7 d, and the time required to reach the platform (escape latency) was measured. As shown in Figure 2*A*, APPsw/WT mice took a significantly longer time than WT/WT mice to reach the platform, a result that is consistent with previous reports (Van Dam et al., 2003) and suggests a deficiency in spatial learning and memory in the former group. This impaired ability of APPsw/WT mice to reach the hidden platform did not reflect reduced swimming ability, as swimming speed and ability to locate a visible platform were indistinguishable between the

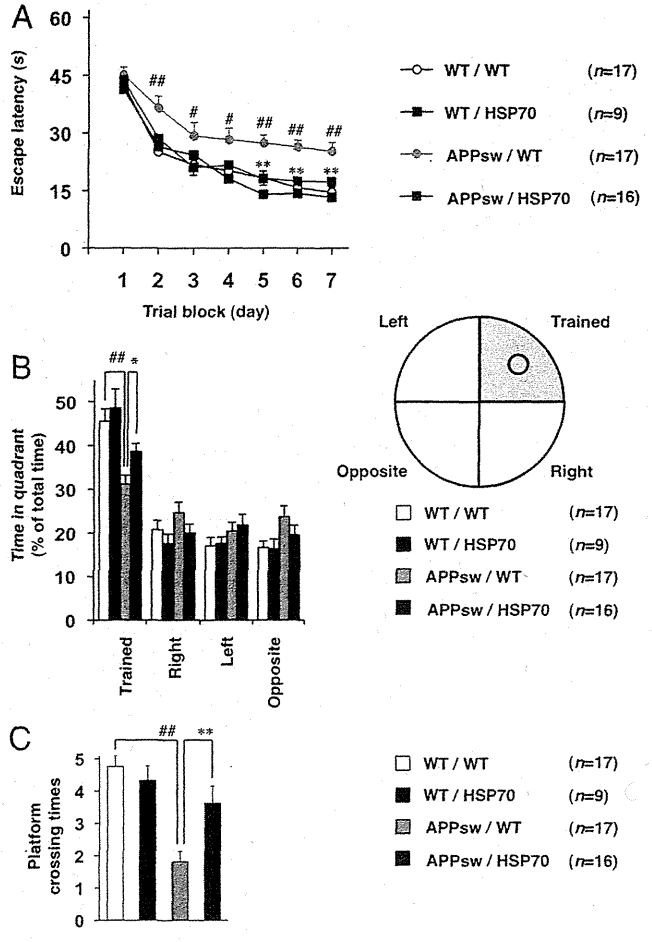

Figure 2. Effects of overexpression of HSP70 on spatial learning and memory in transgenic mice expressing APPsw. Cognitive behavioral tests were performed, using the Morris water maze, on 12-month-old WT/WT (n = 17), WT/HSP70 (n = 9), APPsw/WT (n = 17), and APPsw/HSP70 mice (n = 16) as described in Materials and Methods. The average (4 tests) escape latency in each trial block was measured for 7 d (***A***), after which the mice were subjected to a transfer test in which the platform was removed. ***B***, ***C***, The spatial memory for a platform location was estimated by percentage search time for each quadrant (the platform had been located in the "trained" quadrant) (***B***) or platform crossing times (***C***). Values are given as mean ± SEM. $^{**}p < 0.01$, $^{*}p < 0.05$, versus APPsw/WT mice; $^{\#\#}p < 0.01$, $^{\#}p < 0.05$, versus WT/WT mice.

four strains of mice (data not shown). APPsw/HSP70 mice took a significantly shorter time to reach the platform than APPsw/WT mice (Fig. 2*A*). Furthermore, there was no significant difference in the escape latency between APPsw/HSP70 and WT/WT mice or between WT/HSP70 and WT/WT mice (Fig. 2*A*). These results suggest that expression of APPsw leads to disturbances in spatial learning and memory, an effect that can be ameliorated by overexpression of HSP70.

We next performed a transfer test to estimate the spatial memory of platform location. After a 7 d training period (see above), each mouse was subjected to a Morris water maze test in which the platform was removed and the percentage search time for each quadrant was measured. As shown in Figure 2*B*, the ratio of time spent in the trained quadrant was lower for the APPsw/WT group than for either the WT/WT or the APPsw/HSP70 mice. Furthermore, the crossing time of the area where the platform had been located, another indicator of spatial memory, was lower in the APPsw/WT group than in the WT/WT and APPsw/HSP70 cohorts (Fig. 2*C*). Again, there was no significant difference in these indices between WT/HSP70 and WT/WT mice (Fig. 2*B*, *C*).

These results confirm the notion that overexpression of HSP70 ameliorates the spatial memory deficits of transgenic mice expressing APPsw.

Effect of overexpression of HSP70 on Aβ accumulation and neuronal and synaptic loss in transgenic mice expressing APPsw

The amounts of Aβ40 and Aβ42 in soluble and insoluble brain fractions were compared between APPsw/HSP70 and APPsw/WT mice by sELISA. As shown in Figure 3*A*, the levels of Aβ40 and Aβ42 in both brain fractions were lower in the APPsw/HSP70 group than in the APPsw/WT mice.

We then examined the effect of overexpression of HSP70 on plaque deposition and neurotoxicity in APP23 mice. Because plaque deposition and neurotoxicity (neuronal and synaptic loss) were not observed in APP23 mice at the age of 12 months (data not shown), we used mice at the age of 18 months. At first, we compared the level of Aβ plaque deposition in the brain between APPsw/HSP70 mice and APPsw/WT mice by thioflavin-S staining. As shown in Figure 3, *B* and *C*, the level of Aβ plaque deposition in both the hippocampus and the cerebral cortex was much lower in the APPsw/HSP70 mice than in the APPsw/WT animals. Very little Aβ plaque deposition was observed in WT/WT mice (Fig. 3*B*, *C*).

We then compared the number of neurons in the hippocampal CA3 region of APPsw/HSP70 and APPsw/WT mice by NeuN staining. As shown in Figure 3, *D* and *E*, the number of NeuN-positive cells (neurons) was significantly higher in the WT/WT and APPsw/HSP70 brain sections than in the APPsw/WT tissue, suggesting that Aβ-induced neuronal loss was ameliorated by overexpression of HSP70. We also estimated the number of synapses based on synaptophysin staining. The level of synaptophysin staining was higher in sections from both WT/WT and APPsw/HSP70 mice than from APPsw/WT mice (Fig. 3*F*, *G*), indicating that overexpression of HSP70 suppresses Aβ-induced synaptic loss. Together, the results in Figure 3 suggest that overexpression of HSP70 decreases the level of Aβ and Aβ plaque deposition in the brain and protects it against Aβ-induced neurotoxicity.

Effect of overexpression of HSP70 on the production and oligomerization of Aβ

To understand the molecular mechanism governing the HSP70-mediated decrease in levels of Aβ and Aβ plaque deposition, we examined the effect of overexpression of HSP70 on the production of Aβ. In general, production of Aβ is regulated by either modification of APP or modulation of secretase activity. We first examined the effect of overexpression of HSP70 on the maturation of APP, an essential step in the production of Aβ. The mature (*N*- and *O*-glycosylated) and immature (*N*-glycosylated alone) forms of APP (mAPP and imAPP, respectively) can be separated by SDS-PAGE on the basis of molecular weight (Tomita et al., 1998a). As shown in Figure 4*A*, mAPP and imAPP were detected in transgenic mice expressing APPsw, and the total amount of APP and the ratio of mAPP and imAPP were indistinguishable between APPsw/HSP70 mice and APPsw/WT animals. We also found that overexpression of HSP70 did not affect the level of PS1 (Fig. 4*A*).

Next, we tested the notion that overexpression of HSP70 affects production of Aβ through modulation of secretase activity by comparing the amount of CTFs, the secreted forms of APP that are generated by α or β-secretase (CTFα or CTFβ, respectively, known as an indirect index of the secretase activity), between APPsw/HSP70 and APPsw/WT mice. Under our experimental conditions, we could not detect the band of CTFγ. As shown in Figure 4*B*, CTFα and CTFβ were detected in transgenic mice ex-

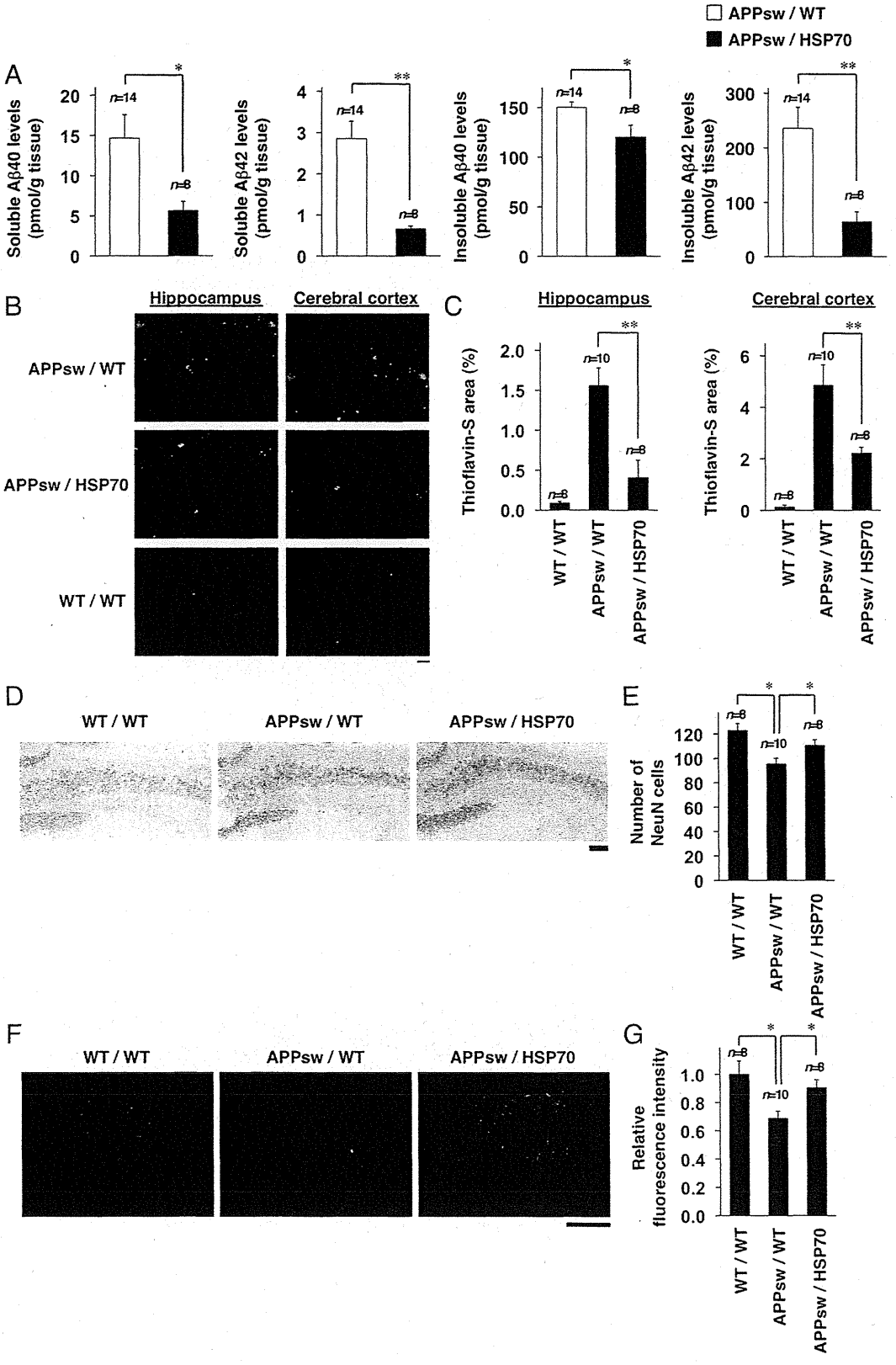

Figure 3. Effects of HSP70 overexpression on Aβ levels, Aβ plaque deposition, and neuronal and synaptic loss in the brain of transgenic mice expressing APPsw. ***A***, Soluble and insoluble fractions were prepared from the brains of 12-month-old APPsw/WT ($n = 14$) and APPsw/HSP70 mice ($n = 8$). The amounts of Aβ40 and Aβ42 in each fraction were determined by sELISA as described in Materials and Methods. ***B***, ***D***, ***F***, Brain sections were prepared from 18-month-old APPsw/WT ($n = 10$), APPsw/HSP70 ($n = 8$), and WT/WT mice ($n = 8$), and then subjected to thioflavin-S staining (***B***) and immunohistochemical analysis with an antibody to NeuN (***D***) or synaptophysin (***F***). Scale bars: ***B***, 200 μm; ***D***, 100 μm; ***F***, 50 μm. ***C***, ***E***, ***G***, Relative area stained with thioflavin-S (***C***), number of NeuN-positive cells in hippocampal CA3 region (***E***), and relative fluorescence intensity (synaptophysin) in hippocampal CA3 region (***G***) (3 sections per brain) were determined. Values are given as mean ± SEM. $^{**}p < 0.01$; $^{*}p < 0.05$.

pressing APPsw, and the amounts of CTFα and CTFβ were indistinguishable between the APPsw/HSP70 and APPsw/WT mice. We then directly measured β- and γ-secretase activity, using the APP-derived fluorescent substrate of each secretase (Hoshino et al., 2009). As shown in Figure 4*C*, the activity was indistinguishable between the APPsw/HSP70 and APPsw/WT groups. These results suggest that overexpression of HSP70 does not affect the production of Aβ.

To test this idea *in vitro*, we prepared primary cultures of neurons from APPsw/HSP70 and APPsw/WT mice and compared the level and modification of APP in the cells, as well as the level of Aβ40 and Aβ42 in the culture medium. We also confirmed the overexpression of HSP70 in primary neurons prepared from APPsw/HSP70 mice (Fig. 4*D*). As shown in Figure 4, *D* and *E*, no significant differences were observed in the total amount of APP, the ratio of mAPP and imAPP, and the levels of Aβ40 and Aβ42 in the primary neuronal cultures between the APPsw/HSP70 and APPsw/WT groups, supporting the idea that overexpression of HSP70 does not affect the production of Aβ.

We then compared the level of Aβ oligomer in the brain of APPsw/HSP70 and APPsw/WT mice by immunoblotting analysis. As shown in Figure 5, *A* and *B*, not only the level of Aβ monomer but also that of Aβ oligomers (dimer, trimer, and hexamer) was lower in the APPsw/HSP70 animals. The decrease in the level of Aβ oligomer in the brain of APPsw/HSP70 was confirmed by ELISA assay for Aβ oligomer (Fig. 5*C*) and dot-blotting assay with antibody that specifically recognizes oligomer form of Aβ (A11) (Fig. 5*D*,*E*). The specificity of this antibody (A11) to Aβ oligomer was suggested by the observation that this antibody did not give positive signals against samples from wild-type mice (without expression of APPsw) (supplemental Fig. 2, available at www.jneurosci.org as supplemental material).

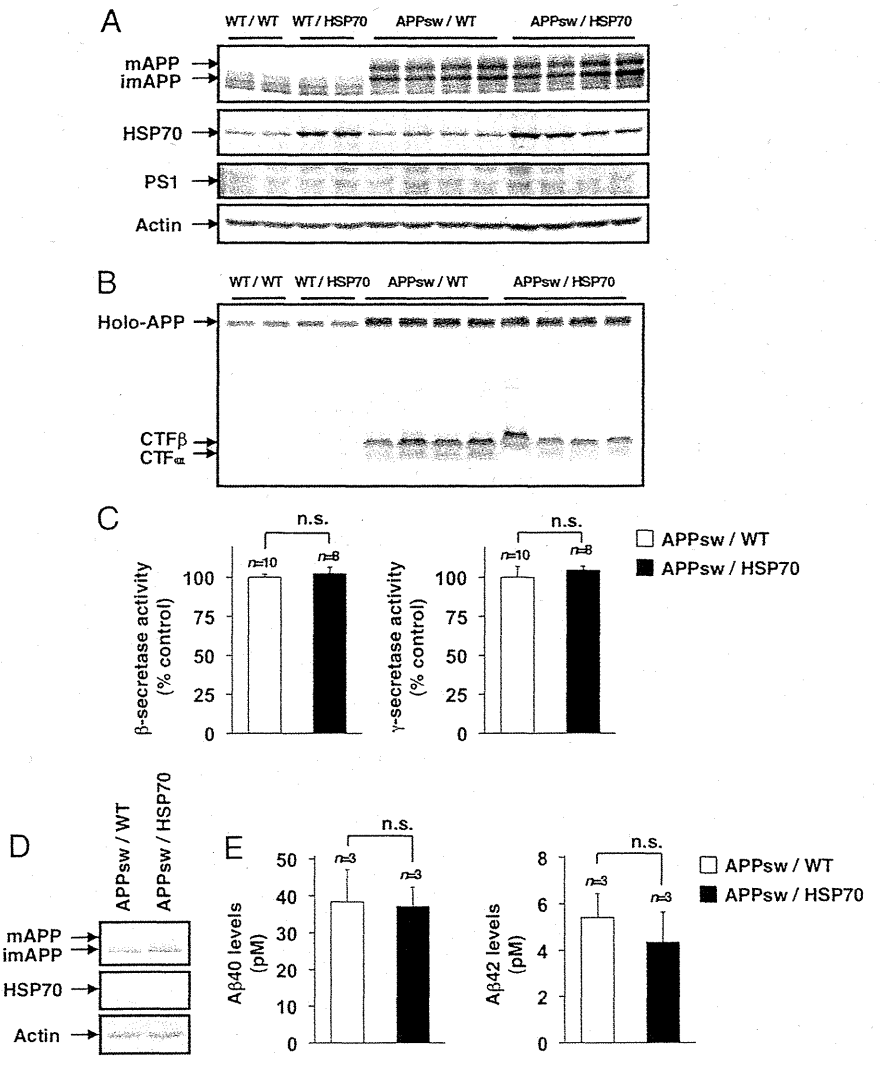

Figure 4. Effects of HSP70 overexpression on the production of Aβ. ***A–C***, Whole-cell extracts (***A***, ***B***) and membrane fractions (***C***) were prepared from the brains of 12-month-old WT/WT, WT/HSP70, APPsw/WT, and APPsw/HSP70 mice. Whole-cell extracts were subjected to immunoblotting with an antibody to APP (***A***, ***B***), HSP70 (***A***), PS1 (***A***), or actin (***A***). Membrane fractions were subjected to a β- or γ-secretase-mediated peptide cleavage assay as described in Materials and Methods [APPsw/WT ($n = 10$) and APPsw/HSP70 mice ($n = 8$)]. Values are given as mean ± SEM. n.s., Not significant (***C***). ***D***, ***E***, Primary neurons prepared from APPsw/WT mice ($n = 3$) and APPsw/HSP70 mice ($n = 3$) were incubated for 7 d. Whole-cell extracts were prepared and subjected to immunoblotting with an antibody to APP, HSP70, or actin (***D***). After incubation for 48 h, the amounts of Aβ40 and Aβ42 in the conditioned medium were determined by sELISA. Values are given as mean ± SD. n.s., Not significant (***E***).

We then examined the colocalization of Hsp70 with APP, Aβ, Aβ oligomer, and Aβ plaque. Intracellular colocalization of HSP70 with APP and Aβ was observed (supplemental Fig. 3*A*,*C*, available at www.jneurosci.org as supplemental material). However, extracellular colocalization of HSP70 with Aβ plaque was not observed so clearly (supplemental Fig. 3*B*,*D*, available at www.jneurosci.org as supplemental material). The intracellular colocalization of HSP70 with Aβ oligomer was also observed in both hippocampus and cerebral cortex (supplemental Fig. 3*E*,*F*, available at www.jneurosci.org as supplemental material).

Effect of overexpression of HSP70 on the expression of genes involving Aβ clearance

As described in Introduction, degradation by enzymes and phagocytosis by microglia and astrocytes are involved in the clearance of Aβ (Miners et al., 2008). We therefore next compared the expression of genes involved in this process. Real-time RT-PCR analysis of brain samples revealed that the mRNA expression of *ide*, but not that of *neprilysin* or *ece-2*, was higher in the APPsw/HSP70 mice than in the APPsw/WT animals (Fig. 6*A*). The upregulation of mRNA expression of *ide* by overexpression of HSP70 was also observed in wild-type mice (without expression of APPsw) (supplemental Fig. 4, available at www.jneurosci.org as supplemental material). We also examined the effect of overexpression of HSP70 on the mRNA expression of *ide* in primary cultures of neurons, astrocytes, and microglia. As shown in Figure 6*B*, the mRNA expression of *ide* was higher in primary astrocyte and microglial cultures prepared from APPsw/HSP70 mice than in those from APPsw/WT mice. In contrast, no significant difference was seen in the neuronal cultures (Fig. 6*B*). These results suggest that the upregulation of *ide* expression is involved in the decrease in the level of Aβ observed in the brain of APPsw/HSP70 mice.

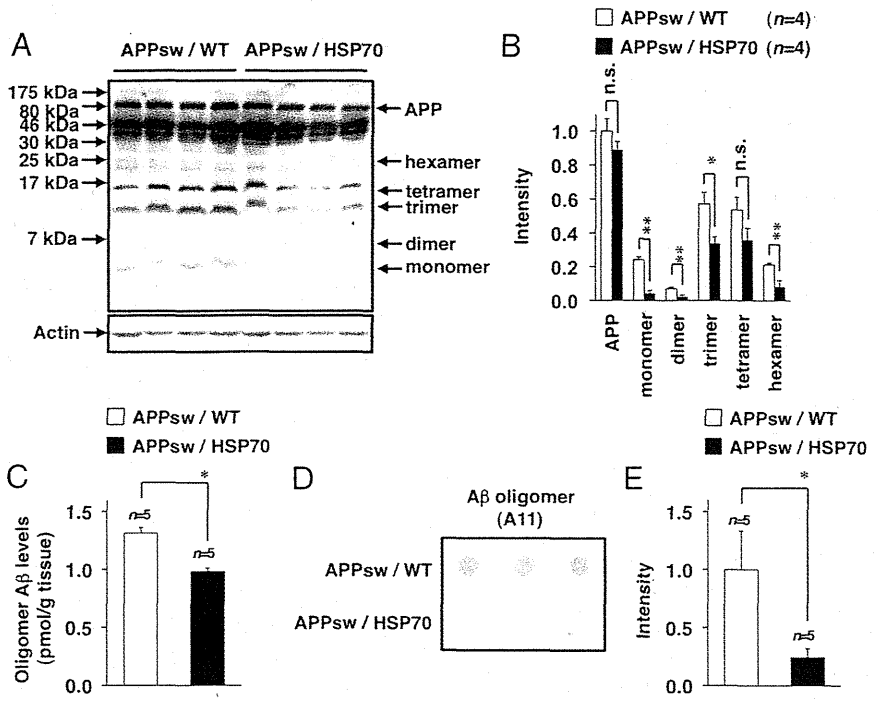

Figure 5. Effects of HSP70 overexpression on the levels of Aβ oligomers in the brains of transgenic mice expressing APPsw. ***A–E***, Whole-cell extracts (***A***, ***B***) or soluble fractions (***C–E***) were prepared from the brains of 12-month-old APPsw/WT and APPsw/HSP70 mice, and then subjected to immunoblotting with an antibody to Aβ (6E10) (***A***), ELISA for Aβ oligomer [APPsw/WT (n = 5) and APPsw/HSP70 mice (n = 5)] (***C***), or dot-blotting assay with an antibody against Aβ oligomer (A11) (***D***). The band intensity of APP and each form of Aβ was determined, corrected with that of actin, and expressed relative to the control [APPsw/WT (n = 4) and APPsw/HSP70 mice (n = 4)] (***B***). The dot intensity was determined and expressed relative to the control (APP in APPsw/WT mice) [APPsw/WT (n = 5) and APPsw/HSP70 mice (n = 5)] (***E***). Values are given as mean ± SEM (***B***, ***C***, ***E***). $^{**}p < 0.01$; $^{*}p < 0.05$. n.s., Not significant.

It has been suggested that inflammation stimulates the progression of the pathogenesis of AD (Wyss-Coray, 2006). However, inflammation also activates the phagocytotic activity of microglia and astrocytes, resulting in stimulation of Aβ clearance (Wyss-Coray et al., 2001). Thus, the relationship between inflammation and progression of AD is complicated, with some proinflammatory cytokines (such as TNF-α) being suggested to promote the progression of AD, whereas others (such as IL-1β and IL-6) have a negative effect in mouse models of the disease (Tesseur et al., 2006; He et al., 2007; Hoshino et al., 2007b; Shaftel et al., 2007). TGF-β1, a key cytokine regulating the response of the brain to injury and inflammation, has also been suggested to suppress the progression of AD. Therefore, we then examined the expression of cytokines that have been suggested to affect the phagocytosis of Aβ (IL-1β, IL-6, TNF-α, and TGF-β1) (Wyss-Coray et al., 2001; Tesseur et al., 2006; He et al., 2007; Hoshino et al., 2007b; Shaftel et al., 2007). As shown in Figure 7*A*, the mRNA expression of *tgf-β1* in the brain was higher in the APPsw/HSP70 mice than in APPsw/WT animals. However, no differences were observed in the mRNA expression of the other cytokines (Fig. 7*A*). Similar results were obtained at the protein level, as judged by ELISA (Fig. 7*B*). The increased mRNA expression of *tgf-β1* and protein level of TGF-β1 by overexpression of HSP70 was also observed in wild-type mice (without expression of APPsw) (supplemental Fig. 4, available at www.jneurosci.org as supplemental material).

We also examined the effect of overexpression of HSP70 on the mRNA expression of *tgf-β1* in primary cultures of neurons, astrocytes, and microglia. As shown in Figure 7*C*, *tgf-β1* mRNA expression was higher in the neuron and astrocyte cultures prepared from APPsw/HSP70 mice than in those from APPsw/WT animals. However, no such difference was observed in the microglial cultures (Fig. 7*C*). Together, these findings suggest that the higher expression of *tgf-β1* is responsible for the lower level of Aβ seen in the brains of APPsw/HSP70 mice, compared with their APPsw/WT counterparts.

Finally, we examined the effect of overexpression of HSP70 on microglial activation by immunohistochemical analysis with an antibody against Iba1 (a marker for activated microglia). As shown in supplemental Figure 5 (available at www.jneurosci.org as supplemental material), the level of Iba1 expression was higher in APPsw/HSP70 mice than APPsw/WT, suggesting that expression of HSP70 activates microglia in APP23 mice.

Discussion

HSPs have attracted considerable attention as AD drug targets because of their unique properties as molecular chaperones (i.e., their ability to unfold and refold abnormal proteins). Other activities of HSPs *in vitro*, such as cytoprotection against Aβ neurotoxicity, suppression of inflammation, and stimulation of Aβ phagocytosis, have increased this attention. Furthermore, the ameliorative effect of HSPs has also been suggested in the case of other neurodegenerative conditions, such as polyglutamine diseases and Parkinson's disease (Adachi et al., 2003; Katsuno et al., 2005; Lo Bianco et al., 2008). Despite this, no *in vivo* evidence exists to support the idea that HSPs are protective in vertebrate AD models. Therefore, in this study, we tested this idea using transgenic mouse strains expressing APPsw and HSP70.

Because AD results in cognitive impairment, it is important to find endogenous factors that affect not only the pathological but also the functional (cognitive) phenotypes in the animal models. This notion is supported by previous reports that some endogenous factors ameliorate cognitive dysfunction in AD model mice without affecting the pathological phenotypes (such as Aβ plaque deposition) (Roberson et al., 2007; Kanninen et al., 2009). In the present study, we found that APPsw/HSP70 mice display a higher level of cognitive function (spatial learning and memory) than APPsw/WT mice, suggesting that overexpression of HSP70 ameliorates the deficits in spatial learning and memory caused by expression of APPsw. Furthermore, we demonstrated that no significant differences in spatial learning and memory exist between WT/WT and WT/HSP70 mice, suggesting that overexpression of HSP70 does not affect the cognitive ability of wild-type mice.

We also found that there are lower levels of Aβ in both the soluble and insoluble fractions of APPsw/HSP70 brains than in those prepared from APPsw/WT mice, suggesting that overexpression of HSP70 suppresses production of Aβ. However, no such differences were observed in the levels of CTFα and CTFβ, indicators of proteolysis by α- or β-secretase, respectively. Furthermore, the activities of β- and γ-secretase in the brain were also indistinguishable between the two strains of mice. These *in vivo* re-

sults suggest that overexpression of HSP70 does not affect the production of Aβ. In fact, we showed that the level of Aβ in the conditioned medium was similar between HSP70-overexpressing neurons and control neurons. Inflammatory factors, such as PGE_2 (prostaglandin E_2) and proinflammatory cytokines, are known to enhance the production of Aβ (Wyss-Coray, 2006; Hoshino et al., 2007b, 2009), and the antiinflammatory activity of HSP70 has recently been reported (Chan et al., 2004; Sun et al., 2005; Tang et al., 2007). However, since expression of proinflammatory cytokines was not affected by overexpression of HSP70 either *in vivo* or *in vitro*, the antiinflammatory activity of HSP70 does not appear to contribute to the ameliorative effect of HSP70 in AD model mice.

As described in Introduction, Aβ is cleared from the brain through enzyme-mediated degradation, phagocytosis by microglia and astrocytes, and transport into the blood and lymph nodes (Miners et al., 2008; Zlokovic, 2008; Rodríguez et al., 2009). The inability of HSP70 to affect the production of Aβ suggests that the clearance of Aβ is enhanced in transgenic mice expressing HSP70. We found that the expression of IDE, an Aβ-degrading enzyme, is enhanced by overexpression of HSP70 both *in vitro* and *in vivo*. We also demonstrated that the expression of TGF-β1 is increased by overexpression of HSP70. Given that it has been reported that TGF-β1 stimulates Aβ clearance through activation of phagocytic microglia (Wyss-Coray et al., 2001) and we here suggested that overexpression of HSP70 activates microglia, we consider that the lower level of Aβ observed in the brains of transgenic mice expressing HSP70 is attributable to the stimulation of Aβ clearance through upregulation of expression of IDE and TGF-β1. In terms of the mechanism underpinning the upregulation of TGF-β1 expression because of overexpression of HSP70, we consider a possibility that extracellular HSP70 is responsible, as it has previously been reported that extracellular HSP70 stimulates the expression of TGF-β1 (Kimura et al., 1998).

However, there is no direct evidence to show that lower levels of Aβ in mice with overexpression of HSP70 is mediated by Aβ-degrading enzyme and TGF-β1, and thus another mechanism may be involved in the phenomenon. For example, Hsp70 might increase the degradation of Aβ by stimulating autophagy or Hsp70 might directly modulate the activity of microglia to degrade Aβ.

The current findings show that the level of Aβ plaque deposition in the brain

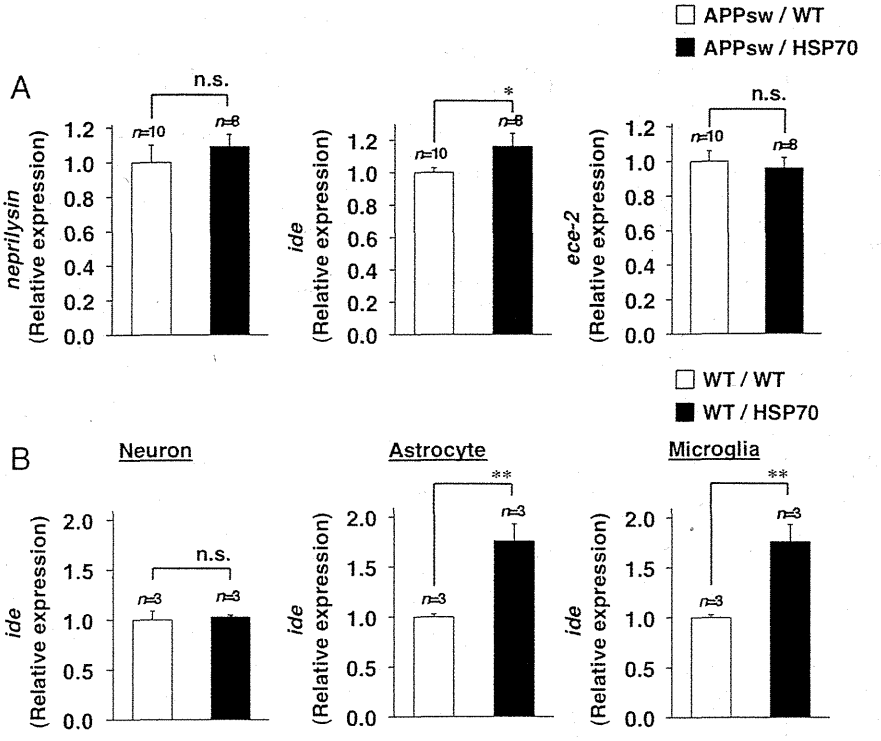

Figure 6. Effects of HSP70 overexpression on the expression of Aβ-degrading enzymes. ***A***, ***B***, Total RNA was extracted from the brains of 12-month-old APPsw/WT ($n = 10$) and APPsw/HSP70 mice ($n = 8$) (***A***) or from primary cultures of neurons, astrocytes and microglia prepared from WT/WT ($n = 3$) and WT/HSP70 mice ($n = 3$) (***B***). RNA samples were subjected to real-time RT-PCR using a specific primer for each gene. Values were normalized to *gapdh* gene expression and expressed relative to the control sample. Values are given as mean ± SEM (***A***) or SD (***B***). $^{**}p < 0.01$; $^{*}p < 0.05$; n.s., not significant.

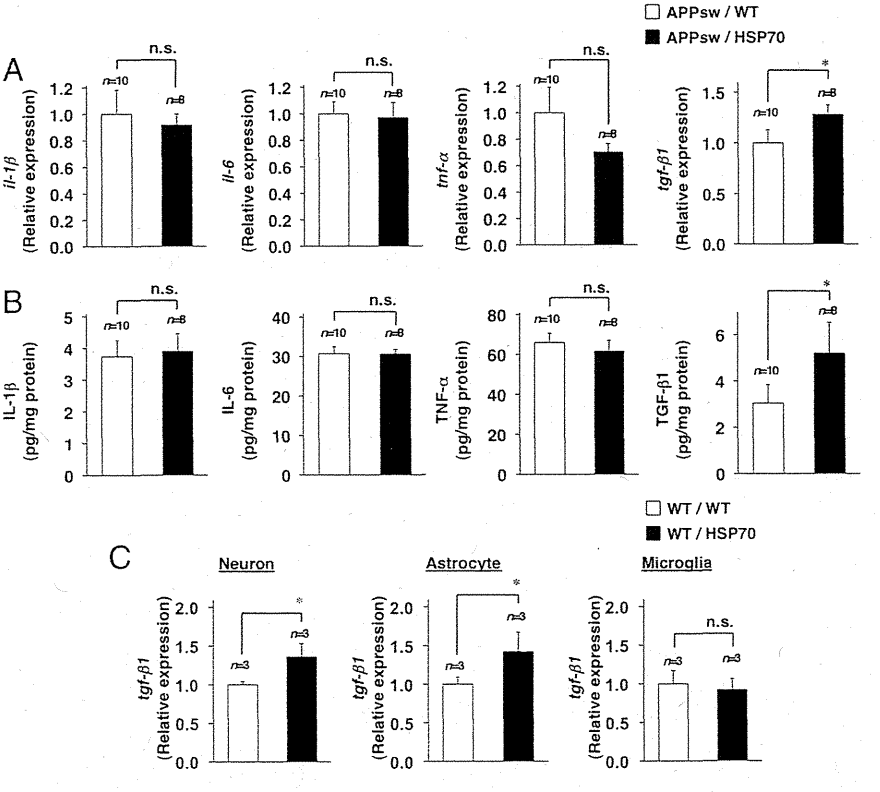

Figure 7. Effects of HSP70 overexpression on cytokine expression. ***A***, ***B***, Total RNA (***A***) or whole-cell extracts (***B***) were prepared from the brains of 12-month-old APPsw/WT ($n = 10$) and APPsw/HSP70 mice ($n = 8$). ***C***, Total RNA was also extracted from primary culture of neurons, astrocytes, and microglia prepared from WT/WT ($n = 3$) and WT/HSP70 mice ($n = 3$). RNA samples were subjected to real-time RT-PCR as described in the legend of Figure 6 (***A***, ***C***). The amounts of cytokine in the whole-cell extracts were determined by ELISA (***B***). Values are given as mean ± SEM (***A***, ***B***) or SD (***C***). $^{*}p < 0.05$. n.s., Not significant.

is reduced in APPsw/HSP70 mice compared with APPsw/WT animals. We also found that the level of Aβ oligomers is lower in the APPsw/HSP70 mouse brain. One explanation of these phenotypes is the lower level of monomeric Aβ in the APPsw/HSP70 mice than in the APPsw/WT animals. However, we believe that the antiaggregation activity of HSP70 for Aβ that was suggested by previous *in vitro* studies (Muchowski and Wacker, 2005; Evans et al., 2006; Kumar et al., 2007; Yoshiike et al., 2008) is involved in these phenotypes. We also found that APPsw/HSP70 mice have less neuronal and synaptic loss than their APPsw/WT counterparts. Again, the phenotype can be explained by the lower level of Aβ. However, we consider that the cytoprotective activity of HSP70 against Aβ-induced neuronal apoptosis that was suggested by previous *in vitro* studies (Magrané et al., 2004) is involved in the phenotype.

As outlined in Introduction, the beneficial effects of HSP70 in animal models of various diseases suggest the potential therapeutic benefit of HSP70 inducers for these conditions (Tanaka et al., 2007, 2010; Asano et al., 2009; Suemasu et al., 2009; Matsuda et al., 2010; Yamashita et al., 2010), a possibility that can now be expanded to include AD based on the results of the present study. A number of recent studies have revealed new molecules that induce HSPs (Kieran et al., 2004; Westerheide et al., 2004; Yan et al., 2004). However, the development of new candidate drugs requires them to pass through the clinical trials process, with the prospect of encountering side effects. In light of this, we have focused our attention on geranylgeranylacetone (GGA). GGA, a leading antiulcer drug on the Japanese market, has been reported to be a nontoxic HSP inducer (Hirakawa et al., 1996). GGA has also been shown to upregulate the expression of HSP70 in various tissues, including the stomach, intestine, liver, heart, eye, ear, skin, lung, and brain (Hirakawa et al., 1996; Ooie et al., 2001; Katsuno et al., 2005; Asano et al., 2009). We and another group have previously reported that GGA suppresses not only gastric lesions but also lesions of the small intestine and inflammatory bowel disease-related colitis (Ohkawara et al., 2005; Asano et al., 2009; Suemasu et al., 2009). Furthermore, we have demonstrated that GGA ameliorates the phenotype in an animal model of spinal and bulbar muscular atrophy (a polyglutamine disease) by suppressing the aggregation of pathogenic proteins (Katsuno et al., 2005). Compared with new molecules that induce HSPs, GGA has an advantage, given that its safety has already been clinically demonstrated. We therefore consider that animal and clinical studies should be performed to prove the effectiveness of GGA for preventing and treating AD.

References

Adachi H, Katsuno M, Minamiyama M, Sang C, Pagoulatos G, Angelidis C, Kusakabe M, Yoshiki A, Kobayashi Y, Doyu M, Sobue G (2003) Heat shock protein 70 chaperone overexpression ameliorates phenotypes of the spinal and bulbar muscular atrophy transgenic mouse model by reducing nuclear-localized mutant androgen receptor protein. J Neurosci 23:2203–2211.

Asano T, Tanaka K, Yamakawa N, Adachi H, Sobue G, Goto H, Takeuchi K, Mizushima T (2009) HSP70 confers protection against indomethacin-induced lesions of the small intestine. J Pharmacol Exp Ther 330:458–467.

Bradford MM (1976) A rapid and sensitive method for the quantitation of microgram quantities of protein utilizing the principle of protein-dye binding. Anal Biochem 72:248–254.

Chan JY, Ou CC, Wang LL, Chan SH (2004) Heat shock protein 70 confers cardiovascular protection during endotoxemia via inhibition of nuclear factor-kappaB activation and inducible nitric oxide synthase expression in the rostral ventrolateral medulla. Circulation 110:3560–3566.

Evans CG, Wisén S, Gestwicki JE (2006) Heat shock proteins 70 and 90 inhibit early stages of amyloid beta-(1–42) aggregation in vitro. J Biol Chem 281:33182–33191.

Farmery MR, Tjernberg LO, Pursglove SE, Bergman A, Winblad B, Näslund J (2003) Partial purification and characterization of gamma-secretase from post-mortem human brain. J Biol Chem 278:24277–24284.

Fukumoto H, Cheung BS, Hyman BT, Irizarry MC (2002) Beta-secretase protein and activity are increased in the neocortex in Alzheimer disease. Arch Neurol 59:1381–1389.

Haass C, Selkoe DJ (2007) Soluble protein oligomers in neurodegeneration: lessons from the Alzheimer's amyloid beta-peptide. Nat Rev Mol Cell Biol 8:101–112.

Hardy J, Selkoe DJ (2002) The amyloid hypothesis of Alzheimer's disease: progress and problems on the road to therapeutics. Science 297:353–356.

He P, Zhong Z, Lindholm K, Berning L, Lee W, Lemere C, Staufenbiel M, Li R, Shen Y (2007) Deletion of tumor necrosis factor death receptor inhibits amyloid beta generation and prevents learning and memory deficits in Alzheimer's mice. J Cell Biol 178:829–841.

Hirakawa T, Rokutan K, Nikawa T, Kishi K (1996) Geranylgeranylacetone induces heat shock proteins in cultured guinea pig gastric mucosal cells and rat gastric mucosa. Gastroenterology 111:345–357.

Hoshino T, Tsutsumi S, Tomisato W, Hwang HJ, Tsuchiya T, Mizushima T (2003) Prostaglandin E2 protects gastric mucosal cells from apoptosis via EP2 and EP4 receptor activation. J Biol Chem 278:12752–12758.

Hoshino T, Nakaya T, Araki W, Suzuki K, Suzuki T, Mizushima T (2007a) Endoplasmic reticulum chaperones inhibit the production of amyloid-beta peptides. Biochem J 402:581–589.

Hoshino T, Nakaya T, Homan T, Tanaka K, Sugimoto Y, Araki W, Narita M, Narumiya S, Suzuki T, Mizushima T (2007b) Involvement of prostaglandin E2 in production of amyloid-beta peptides both in vitro and in vivo. J Biol Chem 282:32676–32688.

Hoshino T, Namba T, Takehara M, Nakaya T, Sugimoto Y, Araki W, Narumiya S, Suzuki T, Mizushima T (2009) Prostaglandin E2 stimulates the production of amyloid-beta peptides through internalization of the EP4 receptor. J Biol Chem 284:18493–18502.

Huang SM, Mouri A, Kokubo H, Nakajima R, Suemoto T, Higuchi M, Staufenbiel M, Noda Y, Yamaguchi H, Nabeshima T, Saido TC, Iwata N (2006) Neprilysin-sensitive synapse-associated amyloid-beta peptide oligomers impair neuronal plasticity and cognitive function. J Biol Chem 281:17941–17951.

Iwata N, Mizukami H, Shirotani K, Takaki Y, Muramatsu S, Lu B, Gerard NP, Gerard C, Ozawa K, Saido TC (2004) Presynaptic localization of neprilysin contributes to efficient clearance of amyloid-β peptide in mouse brain. J Neurosci 24:991–998.

Kanninen K, Heikkinen R, Malm T, Rolova T, Kuhmonen S, Leinonen H, Ylä-Herttuala S, Tanila H, Levonen AL, Koistinaho M, Koistinaho J (2009) Intrahippocampal injection of a lentiviral vector expressing Nrf2 improves spatial learning in a mouse model of Alzheimer's disease. Proc Natl Acad Sci U S A 106:16505–16510.

Katsuno M, Sang C, Adachi H, Minamiyama M, Waza M, Tanaka F, Doyu M, Sobue G (2005) Pharmacological induction of heat-shock proteins alleviates polyglutamine-mediated motor neuron disease. Proc Natl Acad Sci U S A 102:16801–16806.

Kauppinen TM, Swanson RA (2005) Poly(ADP-ribose) polymerase-1 promotes microglial activation, proliferation, and matrix metalloproteinase-9-mediated neuron death. J Immunol 174:2288–2296.

Kieran D, Kalmar B, Dick JR, Riddoch-Contreras J, Burnstock G, Greensmith L (2004) Treatment with arimoclomol, a coinducer of heat shock proteins, delays disease progression in ALS mice. Nat Med 10:402–405.

Kimura Y, Yamada K, Sakai T, Mishima K, Nishimura H, Matsumoto Y, Singh M, Yoshikai Y (1998) The regulatory role of heat shock protein 70-reactive CD4+ T cells during rat listeriosis. Int Immunol 10:117–130.

Kobayashi K, Noda Y, Matsushita N, Nishii K, Sawada H, Nagatsu T, Nakahara D, Fukabori R, Yasoshima Y, Yamamoto T, Miura M, Kano M, Mamiya T, Miyamoto Y, Nabeshima T (2000) Modest neuropsychological deficits caused by reduced noradrenaline metabolism in mice heterozygous for a mutated tyrosine hydroxylase gene. J Neurosci 20:2418–2426.

Kumar P, Ambasta RK, Veereshwarayya V, Rosen KM, Kosik KS, Band H, Mestril R, Patterson C, Querfurth HW (2007) CHIP and HSPs interact with beta-APP in a proteasome-dependent manner and influence Abeta metabolism. Hum Mol Genet 16:848–864.

Lo Bianco C, Shorter J, Régulier E, Lashuel H, Iwatsubo T, Lindquist S,

Aebischer P (2008) Hsp104 antagonizes alpha-synuclein aggregation and reduces dopaminergic degeneration in a rat model of Parkinson disease. J Clin Invest 118:3087–3097.

Magrané J, Smith RC, Walsh K, Querfurth HW (2004) Heat shock protein 70 participates in the neuroprotective response to intracellularly expressed β-amyloid in neurons. J Neurosci 24:1700–1706.

Matsuda M, Hoshino T, Yamashita Y, Tanaka K, Maji D, Sato K, Adachi H, Sobue G, Ihn H, Funasaka Y, Mizushima T (2010) Prevention of UVB radiation-induced epidermal damage by expression of heat shock protein 70. J Biol Chem 285:5848–5858.

Mattson MP (2004) Pathways towards and away from Alzheimer's disease. Nature 430:631–639.

Mima S, Tsutsumi S, Ushijima H, Takeda M, Fukuda I, Yokomizo K, Suzuki K, Sano K, Nakanishi T, Tomisato W, Tsuchiya T, Mizushima T (2005) Induction of claudin-4 by nonsteroidal anti-inflammatory drugs and its contribution to their chemopreventive effect. Cancer Res 65:1868–1876.

Miners JS, Baig S, Palmer J, Palmer LE, Kehoe PG, Love S (2008) Abeta-degrading enzymes in Alzheimer's disease. Brain Pathol 18:240–252.

Morimoto RI, Santoro MG (1998) Stress-inducible responses and heat shock proteins: new pharmacologic targets for cytoprotection. Nat Biotechnol 16:833–838.

Muchowski PJ, Wacker JL (2005) Modulation of neurodegeneration by molecular chaperones. Nat Rev Neurosci 6:11–22.

Ohkawara T, Nishihira J, Takeda H, Miyashita K, Kato K, Kato M, Sugiyama T, Asaka M (2005) Geranylgeranylacetone protects mice from dextran sulfate sodium-induced colitis. Scand J Gastroenterol 40:1049–1057.

Ooie T, Takahashi N, Saikawa T, Nawata T, Arikawa M, Yamanaka K, Hara M, Shimada T, Sakata T (2001) Single oral dose of geranylgeranylacetone induces heat-shock protein 72 and renders protection against ischemia/reperfusion injury in rat heart. Circulation 104:1837–1843.

Perez N, Sugar J, Charya S, Johnson G, Merril C, Bierer L, Perl D, Haroutunian V, Wallace W (1991) Increased synthesis and accumulation of heat shock 70 proteins in Alzheimer's disease. Brain Res Mol Brain Res 11:249–254.

Plumier JC, Ross BM, Currie RW, Angelidis CE, Kazlaris H, Kollias G, Pagoulatos GN (1995) Transgenic mice expressing the human heat shock protein 70 have improved post-ischemic myocardial recovery. J Clin Invest 95:1854–1860.

Plumier JC, Krueger AM, Currie RW, Kontoyiannis D, Kollias G, Pagoulatos GN (1997) Transgenic mice expressing the human inducible Hsp70 have hippocampal neurons resistant to ischemic injury. Cell Stress Chaperones 2:162–167.

Roberson ED, Scearce-Levie K, Palop JJ, Yan F, Cheng IH, Wu T, Gerstein H, Yu GQ, Mucke L (2007) Reducing endogenous tau ameliorates amyloid beta-induced deficits in an Alzheimer's disease mouse model. Science 316:750–754.

Rodríguez JJ, Olabarria M, Chvatal A, Verkhratsky A (2009) Astroglia in dementia and Alzheimer's disease. Cell Death Differ 16:378–385.

Saito Y, Sano Y, Vassar R, Gandy S, Nakaya T, Yamamoto T, Suzuki T (2008) X11 proteins regulate the translocation of amyloid beta-protein precursor (APP) into detergent-resistant membrane and suppress the amyloidogenic cleavage of APP by beta-site-cleaving enzyme in brain. J Biol Chem 283:35763–35771.

Shaftel SS, Kyrkanides S, Olschowka JA, Miller JN, Johnson RE, O'Banion MK (2007) Sustained hippocampal IL-1 beta overexpression mediates chronic neuroinflammation and ameliorates Alzheimer plaque pathology. J Clin Invest 117:1595–1604.

Sturchler-Pierrat C, Abramowski D, Duke M, Wiederhold KH, Mistl C, Rothacher S, Ledermann B, Bürki K, Frey P, Paganetti PA, Waridel C, Calhoun ME, Jucker M, Probst A, Staufenbiel M, Sommer B (1997) Two amyloid precursor protein transgenic mouse models with Alzheimer disease-like pathology. Proc Natl Acad Sci U S A 94:13287–13292.

Suemasu S, Tanaka K, Namba T, Ishihara T, Katsu T, Fujimoto M, Adachi H, Sobue G, Takeuchi K, Nakai A, Mizushima T (2009) A role for HSP70 in protecting against indomethacin-induced gastric lesions. J Biol Chem 284:19705–19715.

Sun D, Chen D, Du B, Pan J (2005) Heat shock response inhibits NF-kappaB activation and cytokine production in murine Kupffer cells. J Surg Res 129:114–121.

Tanaka K, Namba T, Arai Y, Fujimoto M, Adachi H, Sobue G, Takeuchi K, Nakai A, Mizushima T (2007) Genetic evidence for a protective role for heat shock factor 1 and heat shock protein 70 against colitis. J Biol Chem 282:23240–23252.

Tanaka K, Ishihara T, Azuma A, Kudoh S, Ebina M, Nukiwa T, Sugiyama Y, Tasaka Y, Namba T, Ishihara T, Sato K, Mizushima Y, Mizushima T (2010) Therapeutic effect of lecithinized superoxide dismutase on bleomycin-induced pulmonary fibrosis. Am J Physiol Lung Cell Mol Physiol 298:L348–L360.

Tang D, Kang R, Xiao W, Wang H, Calderwood SK, Xiao X (2007) The anti-inflammatory effects of heat shock protein 72 involve inhibition of high-mobility-group box 1 release and proinflammatory function in macrophages. J Immunol 179:1236–1244.

Tesseur I, Zou K, Esposito L, Bard F, Berber E, Can JV, Lin AH, Crews L, Tremblay P, Mathews P, Mucke L, Masliah E, Wyss-Coray T (2006) Deficiency in neuronal TGF-beta signaling promotes neurodegeneration and Alzheimer's pathology. J Clin Invest 116:3060–3069.

Tomita S, Kirino Y, Suzuki T (1998a) Cleavage of Alzheimer's amyloid precursor protein (APP) by secretases occurs after O-glycosylation of APP in the protein secretory pathway. Identification of intracellular compartments in which APP cleavage occurs without using toxic agents that interfere with protein metabolism. J Biol Chem 273:6277–6284.

Tomita S, Kirino Y, Suzuki T (1998b) A basic amino acid in the cytoplasmic domain of Alzheimer's beta-amyloid precursor protein (APP) is essential for cleavage of APP at the alpha-site. J Biol Chem 273:19304–19310.

Van Dam D, D'Hooge R, Staufenbiel M, Van Ginneken C, Van Meir F, De Deyn PP (2003) Age-dependent cognitive decline in the APP23 model precedes amyloid deposition. Eur J Neurosci 17:388–396.

Wang J, Ho L, Chen L, Zhao Z, Zhao W, Qian X, Humala N, Seror I, Bartholomew S, Rosendorff C, Pasinetti GM (2007) Valsartan lowers brain beta-amyloid protein levels and improves spatial learning in a mouse model of Alzheimer disease. J Clin Invest 117:3393–3402.

Westerheide SD, Bosman JD, Mbadugha BN, Kawahara TL, Matsumoto G, Kim S, Gu W, Devlin JP, Silverman RB, Morimoto RI (2004) Celastrols as inducers of the heat shock response and cytoprotection. J Biol Chem 279:56053–56060.

Wyss-Coray T (2006) Inflammation in Alzheimer disease: driving force, bystander or beneficial response? Nat Med 12:1005–1015.

Wyss-Coray T, Lin C, Yan F, Yu GQ, Rohde M, McConlogue L, Masliah E, Mucke L (2001) TGF-beta1 promotes microglial amyloid-beta clearance and reduces plaque burden in transgenic mice. Nat Med 7:612–618.

Yamashita Y, Hoshino T, Matsuda M, Kobayashi C, Tominaga A, Nakamura Y, Nakashima K, Yokomizo K, Ikeda T, Mineda K, Maji D, Niwano Y, Mizushima T (2010) HSP70 inducers from Chinese herbs and their effect on melanin production. Exp Dermatol 19:e340–e342.

Yan D, Saito K, Ohmi Y, Fujie N, Ohtsuka K (2004) Paeoniflorin, a novel heat shock protein-inducing compound. Cell Stress Chaperones 9:378–389.

Yoshiike Y, Minai R, Matsuo Y, Chen YR, Kimura T, Takashima A (2008) Amyloid oligomer conformation in a group of natively folded proteins. PLoS One 3:e3235.

Zlokovic BV (2008) The blood-brain barrier in health and chronic neurodegenerative disorders. Neuron 57:178–201.

Biochemical Pharmacology 81 (2011) 1124–1135

Contents lists available at ScienceDirect

Biochemical Pharmacology

journal homepage: www.elsevier.com/locate/biochempharm

Acetaminophen-induced differentiation of human breast cancer stem cells and inhibition of tumor xenograft growth in mice

Masaya Takehara, Tatsuya Hoshino, Takushi Namba, Naoki Yamakawa, Tohru Mizushima *

Graduate School of Medical and Pharmaceutical Sciences, Kumamoto University, 5-1, Oe-honmachi, Kumamoto 862-0973, Japan

ARTICLE INFO

Article history:
Received 13 December 2010
Accepted 22 February 2011
Available online 1 March 2011

Keywords:
Cancer stem cells
Differentiation
Acetaminophen
Anti-cancer drug

ABSTRACT

It is now believed that cancer stem cells (CSCs) that are resistant to chemotherapy due to their undifferentiated nature drive tumor growth, metastasis and relapse, so development of drugs that induce differentiation of CSCs should have a profound impact on cancer eradication. In this study, we screened medicines that are already in clinical use for drugs that induce differentiation of CSCs. We used MDA-MB-231, a human breast cancer cell line that contains cancer stem cell-like cells. We found that acetaminophen, an anti-inflammatory, antipyretic and analgesic drug, induces differentiation of MDA-MB-231 cells. Differentiation was assessed by observing alterations in cell shape and expression of differentiated and undifferentiated cell markers, a decrease in cell invasion activity and an increase in susceptibility to anti-tumor drugs. This increased susceptibility seems to involve suppression of expression of multidrug efflux pumps. We also suggest that this induction of differentiation is mediated by inhibition of a Wnt/β-catenin canonical signaling pathway. Treatment of MDA-MB-231 cells with acetaminophen *in vitro* resulted in the loss of their tumorigenic ability in nude mice. Furthermore, administration of acetaminophen inhibited the growth of tumor xenografts of MDA-MB-231 cells in both the presence and absence of simultaneous administration of doxorubicine, a typical anti-tumor drug for breast cancer. Analysis with various acetaminophen derivatives revealed that *o*-acetamidophenol has a similar differentiation-inducing activity and a similar inhibitory effect on tumor xenograft growth. These results suggest that acetaminophen may be beneficial for breast cancer chemotherapy by inducing the differentiation of CSCs.

1. Introduction

Despite the monoclonal origins of cancers, they are composed of heterogeneous populations of cells with different proliferative, differentiative and tumorigenic properties [1]. To explain this, the cancer stem cell (CSC) hypothesis is proposed: within a given tumor there is a small population of cells that have the capacity to behave like stem cells; in other words they are able to self-renew and are pluripotent, and thus they give rise to heterogeneous tumor phenotypes [2,3]. The existence of CSCs was first proven in the context of acute myelogenous leukemia and subsequently verified in breast, brain, prostate, colon and pancreatic cancers [4–9]. Such studies have also identified an expression profile of cell surface markers that is characteristic of CSCs in each tissue and organ. For example, it has been reported that breast cancer cells that express a high level of clusters of differentiation (CD)-44 and a low or undetectable level of CD24 ($CD44^+/CD24^{-/low}$) have CSC properties [5].

Mortality from cancers remains high due to their resistance to chemo- and radiotherapy, metastasis and relapse. It is now believed that CSCs play important roles in these events. For example, $CD44^+/CD24^{-/low}$ breast cancer cells have higher levels of tumorigenic and metastatic activity *in vivo* and higher levels of invasion, migration, proliferation and anchorage-independent colony formation, than relatively differentiated cells ($CD44^{-/low}/CD24^+$) [5,10–12]. CSCs are also resistant to chemo- and radiotherapy [13–17]. Therefore, chemotherapy kills the bulk of tumor cells but is not so effective at killing CSCs, which survive to regenerate new tumors (relapse) after a period of latency [18,19]. Supporting this notion, it has recently been reported that chemotherapy of primary breast cancer patients increases the level of $CD44^+/CD24^{-/low}$ cells in cancer core biopsies [18,20]. It has also been reported that the level of $CD44^+/CD24^{-/low}$ cells in breast tumors correlates with the poor efficacy of chemo- and radiotherapy [16,18]. Therefore, drugs that specifically and effectively kill CSCs would be beneficial for the treatment of cancers and recently such compounds have been reported [18,21,22]. Alternatively,

* Corresponding author. Tel.: +81 96 371 4323; fax: +81 96 371 4323.
E-mail addresses: mt0125@gpo.kumamoto-u.ac.jp (M. Takehara), thoshino@gpo.kumamoto-u.ac.jp (T. Hoshino), takushi@kumamoto-u.ac.jp (T. Namba), bananao@gpo.kumamoto-u.ac.jp (N. Yamakawa), mizu@gpo.kumamoto-u.ac.jp (T. Mizushima).

0006-2952/$ – see front matter © 2011 Elsevier Inc. All rights reserved.
doi:10.1016/j.bcp.2011.02.012

drugs that induce differentiation of CSCs may also be therapeutically important because such drugs would convert CSCs to be more susceptible to chemotherapy and less active in metastasis. However, chemicals that induce differentiation of CSCs have not yet been reported.

In order to modulate the stem cell-like properties of CSCs, it is important to understand the molecular mechanisms which maintain these properties. Recent studies suggest that these mechanisms may be common both to CSCs and normal stem cells [23]. In breast CSCs and mammary gland stem cells, various signaling pathways, such as the Wnt/β-catenin canonical pathway and the transforming growth factor-β (TGF-β) pathway, play important roles in the maintenance of stem cell-like properties [24–28]. In the Wnt/β-catenin canonical signaling pathway, the binding of Wnt ligands to their receptors inhibits the activity of a multiprotein complex that includes glycogen synthase kinase 3β (GSK3β). This complex phosphorylates β-catenin to target it for ubiquitination and proteolysis. Therefore, when Wnt signal transduction is activated, β-catenin accumulates in the cytosol and some part of this protein translocates to the nucleus. In the nucleus, β-catenin binds to T-cell factor/lymphoid enhancing factor 1 (Tcf/Lef1) family proteins to regulate the transcription of specific genes, including those important for the maintenance of stem cell-like properties (such as *snail*) [25,28,29]. On the other hand, aberrant activation of the Wnt/β-catenin canonical pathway is one of the most frequent signaling abnormalities known in human cancers and it has also been reported that β-catenin is abnormally stabilized in over 50% of breast carcinomas [25]. These data suggests that the Wnt/β-catenin canonical pathway plays an important role in the maintenance of the stem cell-like properties of breast CSCs. In fact, recently, it has been reported in breast CSCs and mammary gland stem cells that activation or inhibition of the Wnt/β-catenin canonical pathway has positive or negative effects on maintenance of their properties of self-renewal and pluripotency [26,30,31]. Therefore, compounds that inhibit this pathway may be beneficial for cancer chemotherapy.

Acetaminophen (AAP) is one of the most widely used over-the-counter anti-inflammatory, antipyretic and analgesic drugs available worldwide. The advantage of this drug is that it has less gastrointestinal toxicity than other anti-inflammatory drugs, such as non-steroidal anti-inflammatory drugs (NSAIDs). On the other hand, the disadvantage of this drug is that it induces hepatotoxicity, causing hepatic centrilobular necrosis [32]. Although discovered more than 100 years ago and used extensively for a long period, the mode of action for its anti-inflammatory, antipyretic and analgesic effects is still unclear. The anti-inflammatory action of NSAIDs is mediated via their inhibitory effect on cyclooxygenase (COX) activity and the synthesis of prostaglandins (PGs), which have a strong capacity to induce inflammation. Although the anti-inflammatory, antipyretic and analgesic actions of AAP resemble those of NSAIDs, in the past it has been believed that this drug acts centrally and is a weak inhibitor of COX [33]; however, this idea is not supported by later studies [34,35]. It was recently suggested that this weak inhibition of COX by AAP is responsible for its anti-inflammatory effect [36]. It seems that COX-inhibition and decreases in the level of PGs play some roles in the anti-inflammatory, antipyretic and analgesic effects of AAP.

In this study, we screened compounds that induce differentiation of CSCs. We used a human breast cancer cell line, MDA-MB-231 cells, which were recently reported to contain mainly (about 80%) $CD44^+/CD24^{-/low}$ cells (cancer stem cell-like cells) [10,11]. Also, it has been reported that the $CD44^+/CD24^{-/low}$ subpopulation of MDA-MB-231 cells has higher levels of growth, anchorage-independent colony formation, adhesion, migration and invasion *in vitro*, and tumorigenicity *in vivo*, than its $CD44^{-/low}/CD24^+$ subpopulation [10]. As for the chemical library for screening, we originally prepared a chemical library containing about 250 medicines already in clinical use. We found that AAP induces differentiation of MDA-MB-231 cells through inhibition of the Wnt/β-catenin canonical signaling pathway. We also found that treatment of MDA-MB-231 cells with AAP *in vitro* resulted in the loss of their tumorigenic ability in nude mice and that administration of AAP inhibited the growth of tumor xenografts of MDA-MB-231 cells both in the presence and absence of the simultaneous administration of doxorubicine. Analysis of various acetaminophen derivatives revealed that *o*-acetamidophenol has similar differentiation-inducing activity and inhibitory effects on tumor xenograft growth, compared to acetaminophen. These results suggest that AAP could be effective for breast cancer therapy through the induction of differentiation of CSCs.

2. Materials and methods

2.1. Chemicals and animals

Dulbecco's modified Eagle's medium (DMEM) was obtained from Nissui Pharmaceutical Co. (Tokyo, Japan). Fetal bovine serum (FBS), G418, LY364947, 3-(4,5-dimethyl-thiazol-2-yl)-2,5-diphenyl tetrazolium bromide (MTT), crystal violet, BSA and 6-bromoindirubin-3′-oxime (BIO) were purchased from Sigma (St. Louis, MO), and lipofectamine (TM2000) and pcDNA3.1(−) were from Invitrogen (Carlsbad, CA). The RNeasy kit was obtained from Qiagen (Valencia, CA), the first-strand cDNA synthesis kit came from TAKARA Bio (Ohtsu, Japan) and iQ SYBR Green Supermix was from Bio-Rad (Hercules, CA). Calcein acet-oxymethyl ester (calcein-AM) and Hepes were from DOJINDO (Kumamoto, Japan). Matrigel was from BD Biosciences (San Jose, CA) and 24-well transwells were from Costar (Lowell, MA). Transaminase C II-test$_{Wako}$, methanol, paraformaldehyde and streptomycin were from Wako Pure Chemical Industries (Tokyo, Japan). The enzyme immunoassay (EIA) kit for PGE_2 was obtained from Cayman (Ann Arbor, MI). An antibody against claudin-1 was from Zymed (San Francisco, CA) and an antibody against actin was from Santa Cruz Biotechnology (Santa Cruz, CA). Fluorescein isothiocyanate (FITC)-conjugated anti-CD44 (clone G44-26) antibody, phycoerythrin (PE)-conjugated anti-CD24 antibody (clone ML5) and an antibody against β-catenin were obtained from BD Biosciences (San Jose, CA). An antibody against CD24 (clone SN3) was from Lab Vision (Fremont, CA). Alexa Fluor 594 goat anti-mouse IgG was obtained from Invitrogen (Carlsbad, CA). Mounting medium for immunohistochemical analysis (VECTASHIELD) was from Vector Laboratories (Burlingame, CA). Penicillin was from MEIJI SEIKA KAISHA, LTD. (Tokyo, Japan). Female ICR wild-type mice and nude mice (Crlj:CD1-*Foxn1*^{nu} mice) (4–6 weeks old) were from Charles River (Kanagawa, Japan). The experiments and procedures described here were carried out in accordance with the Guide for the Care and Use of Laboratory Animals as adopted and promulgated by the National Institutes of Health, and were approved by the Animal Care Committee of Kumamoto University.

2.2. Cell culture and plasmid construction

MDA-MB-231 and MCF-7 (breast cancer cell lines) cells were obtained from ATCC (Manassas, VA). The cells were cultured in DMEM containing 10% FBS, 100 U/ml penicillin and 100 μg/ml streptomycin in a humidified atmosphere of 95% air with 5% CO_2 at 37 °C.

Determination of PGE_2 levels in culture media was done by EIA as previously described [37]. We used a MTT assay for determining viable cell numbers, as described previously [37]. Briefly, cells were incubated for 2 h with MTT solution at a final concentration of 0.5 mg/ml. Isopropanol and hydrochloric acid were added to the

culture medium at final concentrations of 50% and 20 mM, respectively. The optical density of each sample at 570 nm was determined spectrophotometrically using a reference wavelength of 630 nm.

Full-length human cDNA for junctional adhesion molecule A (JAM-A) was prepared by PCR and cloned into pcDNA3.1(−) to create a plasmid for its overexpression. Transfection of MDA-MB-231 cells with the plasmid was carried out using Lipofectamine (TM2000) according to the manufacturer's protocol. The stable transfectants overexpressing JAM-A were selected by real-time RT-PCR analysis. Positive clones were maintained in the presence of 400 μg/ml G418.

2.3. Real-time RT-PCR analysis

Total RNA was extracted using an RNeasy kit according to the manufacturer's protocol. Samples (1 μg RNA) were reverse-transcribed using a first-strand cDNA synthesis kit according to the manufacturer's instructions. Synthesized cDNA was used in real-time RT-PCR (Chromo 4 instrument; Bio-Rad, Hercules, CA) experiments using iQ SYBR GREEN Supermix, and analyzed with Opticon Monitor Software according to the manufacturer's instructions. Specificity was confirmed by electrophoretic analysis of the reaction products and by inclusion of template- or reverse transcriptase-free controls. To normalize the amount of total RNA present in each reaction, *actin* cDNA was used as an internal standard. Primer sequences are available upon request.

2.4. Immunoblotting analysis

Whole cell extracts were prepared as described previously [38]. The protein concentrations of the samples were determined by the Bradford method [39]. Samples were applied to 10% polyacrylamide gels containing SDS, subjected to electrophoresis, and the proteins then immunoblotted with each antibody.

2.5. Analysis of expression of cell surface markers by fluorescence activated cell sorting (FACS)

Cells (5×10^5) were incubated with FITC-conjugated anti-CD44 antibody and PE-conjugated anti-CD24 antibody. Samples were analyzed with a FACSCalibur flow cytometer (Becton Dickinson, Franklin Lakes, NJ). Acquisition of events was stopped at 30,000.

2.6. Calcein-AM accumulation assay

The drug efflux activity in cells was estimated by a calcein-AM accumulation assay as described previously [40], with some modifications. Cells (1×10^6) treated with trypsine were suspended in DMEM containing 2% FBS, 10 mM Hepes and 1 μM calcein-AM and incubated for 10 min at 37 °C. After centrifugation and re-suspension in PBS, the green fluorescence intensity of each sample was measured using a FACSCalibur flow cytometer (Becton Dickinson, Franklin Lakes, NJ). Acquisition of events was stopped at 30,000.

2.7. Cell invasion assay

Cell invasion activity was measured by a transwell matrigel invasion assay as described previously [38], with some modifications. Serum-free DMEM containing 5 mg/ml matrigel was applied to the upper chamber of a 24-well transwell and incubated at 37 °C for 4 h. The cell suspension was applied to the matrigel and the lower chamber was filled with DMEM containing 10% FBS. The plate was incubated at 37 °C for 24 h. Cells were removed from the upper surface of the membrane and the lower surface of the membrane was stained for 10 min with 0.5% crystal violet in 25% methanol, rinsed with distilled water and air-dried overnight. The crystal violet was then extracted with 0.1 M sodium citrate in 50% ethanol and the absorbance was measured at 585 nm.

2.8. Immunostaining

MDA-MB-231 cells were grown in a Lab-Tek II chamber slide system (Nalge Nunc International, Rochester, NY). Cells were fixed in 1% paraformaldehyde for 20 min and blocked in PBS containing 3% BSA for 30 min. The samples were then incubated with each primary antibody. After washing, samples were incubated with the respective secondary antibody conjugated with Alexa Fluor 594 (Molecular Probes, Eugene, OR). Images were captured on a confocal laser-scanning fluorescence microscope (Olympus FV500, Olympus, Tokyo, Japan).

2.9. Evaluation of liver injury

Liver injury was evaluated by measuring the catalytic activities of aspartate aminotransferase (AST) and alanine aminotransferase (ALT) in plasma by use of a transaminase C II-test$_{Wako}$ according to the manufacturer's instructions.

2.10. Assay for tumor xenograft growth

Cells (1×10^7, suspension in 0.2 ml of serum-free DMEM) were subcutaneously inoculated into the right hind footpad of each nude mouse. Tumors were measured weekly using calipers and their volumes were calculated using the following standard formula: width^2 × length × 0.5.

2.11. Immunohistochemical analysis

Tumor xenografts were embedded in OCT compound (Sakura Finetechnical Co., Tokyo, Japan) and cryosectioned. Sections were blocked with 3% goat serum for 15 min, incubated for 12 h with each primary antibody in the presence of 2.5% BSA, and finally incubated for 3 h with Alexa Fluor 594 goat anti-mouse IgG (except for detection of CD44). Samples were mounted with VECTASHIELD and inspected using fluorescence microscopy (Olympus BX51, Olympus, Tokyo, Japan).

2.12. Statistical analysis

All values are expressed as the mean ± S.D. or S.E.M. Two-way analysis of variance (ANOVA) followed by the Tukey test was used to evaluate differences between more than three groups. Differences were considered to be significant for values of $P < 0.05$.

3. Results

3.1. Identification of AAP as a drug inducing differentiation of MDA-MB-231 cells

At first, from about 250 medicines already in clinical use (supplemental Table S1), we screened for drugs that induce differentiation of MDA-MB-231 cells. It has been reported that undifferentiated ($CD44^+/CD24^{-/low}$) or differentiated ($CD44^{-/low}/CD24^+$) breast cancer cells show a dispersed spindle-shaped mesenchymal cell structure or a cobble-stone-like epithelial monolayer structure, respectively [24,28]. Thus, we searched for drugs that induced morphological change of MDA-MB-231 cells (from a mesenchymal cell structure to a cobble-stone-like structure) after treatment for 4 days and found that AAP induces such morphological change (Fig. 1A). This morphological change was

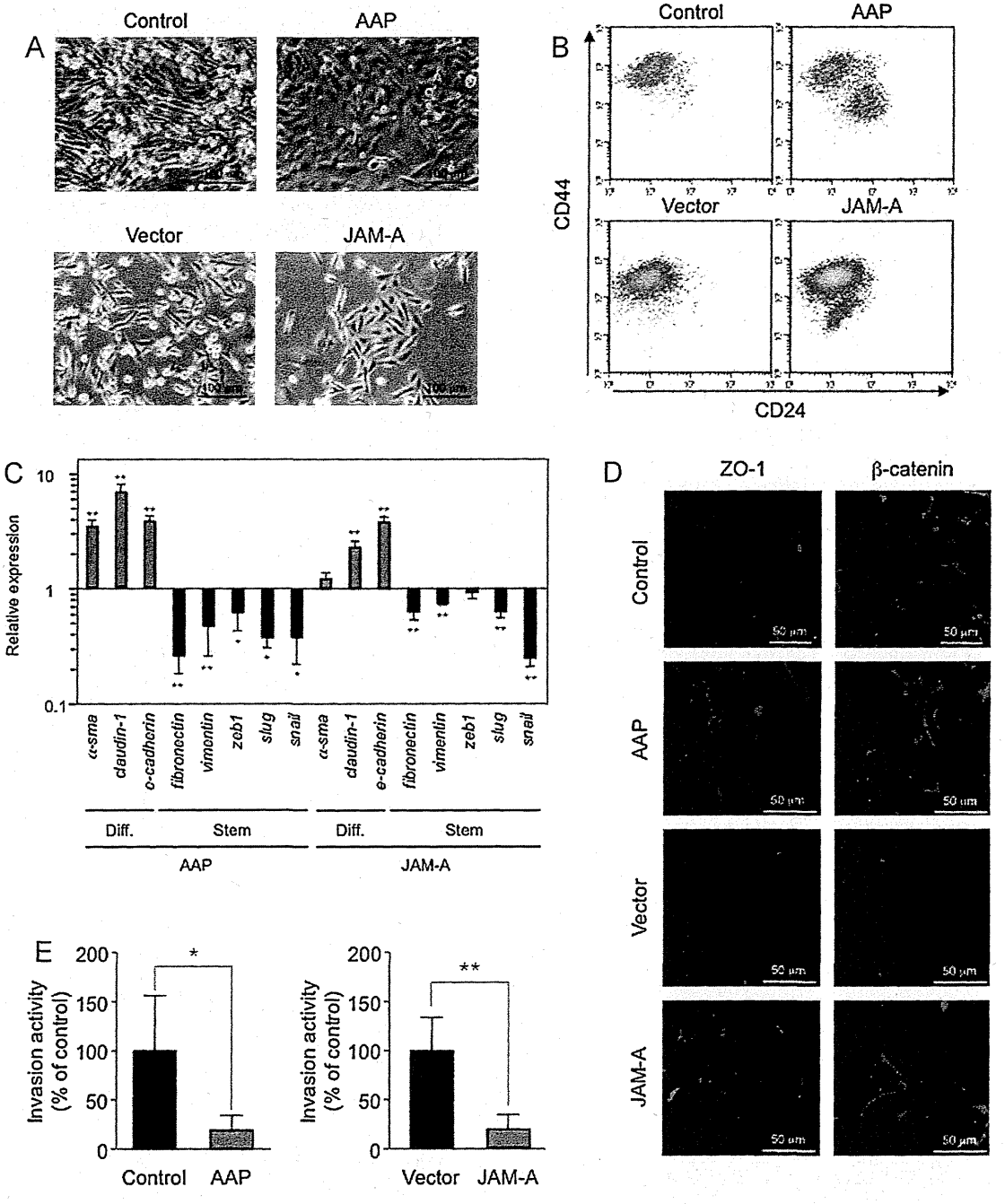

Fig. 1. *AAP-induced differentiation of MDA-MB-231 cells. MDA-MB-231 cells treated with (AAP) and without (Control) 1 mM AAP for 4 days or cells stably transfected with the expression plasmid for JAM-A (JAM-A) or empty vector (Vector) were analyzed (A–E). Cell morphology was examined by phase-contrast microscopic observation (A). Cell surface expression of CD24 and CD44 was analyzed by FACS as described in Section 2 (B). Total RNA was extracted and subjected to real-time RT-PCR using a specific primer set for each gene (Diff, markers for differentiated cells; Stem, markers for stem cells). Values were normalized to the actin gene, expressed relative to the control (C). Expression of ZO-1 and β-catenin was monitored by an immunostaining assay (D). Cell invasion activity was measured on matrigel-coated transwells as described in Section 2 and is expressed relative to the control (E). Values shown are mean ± S.D. ($n = 3–7$). $^{*}P < 0.05$; $^{**}P < 0.01$.*

irreversible: the cell shape was maintained after incubation in AAP-free medium for at least 2 days (data not shown). It has been reported that overexpression of JAM-A, a tight junction protein, in MDA-MB-231 cells induces such morphological change and inhibits cell invasion activity [41], suggesting that overexpression of JAM-A induces differentiation of MDA-MB-231 cells. We confirmed that overexpression of JAM-A induces such morphological changes (Fig. 1A) and we then used JAM-A-overexpressing MDA-MB-231 cells as a positive control in the following experiments. As described above, MDA-MB-231 cells was reported to contain a main subpopulation of $CD44^{+}/CD24^{-/low}$ cells and a minor subpopulation of $CD44^{-/low}/CD24^{+}$ cells [10,11]; we confirmed this by flow cytometry analysis of the surface expression of CD44 and CD24 (Fig. 1B). Furthermore, we found that either treatment with AAP or overexpression of JAM-A in MDA-MB-231 cells decreases the number of $CD44^{+}/CD24^{-/low}$ cells and increases the number of $CD44^{-/low}/CD24^{+}$ cells (Fig. 1B).

It was reported that the subpopulation of $CD44^{+}/CD24^{-/low}$/high aldehyde dehydrogenase $(ALDH)^{+}$ has much high tumorigenicity *in vivo* than $CD44^{+}/CD24^{-/low}/ALDH^{-}$ [42]. As shown in supplemental Fig. S1, treatment of cells with AAP decreased the number of $ALDH^{+}$ cells.

We also examined the mRNA expression of markers for differentiated cells (α-smooth muscle actin (α-SMA), claudin-1

and E-cadherin) and stem cells (fibronectin, vimentin, zinc finger E-box binding homeobox 1 (ZEB-1), Slug and Snail), referring to data in previous reports [24,28,43]. As shown in Fig. 1C, treatment with AAP and overexpression of JAM-A in MDA-MB-231 cells up-regulated or down-regulated mRNA expression of markers for differentiated cell or stem cell-like cells, respectively. It was recently reported that zonula occludens-1 (ZO-1), which localizes cell–cell contacts in differentiated epithelial cells, localizes broadly in the cytosol of MDA-MB-231 cells, and overexpression of JAM-A causes translocation of the protein to cell–cell contacts [41]. By immunostaining analysis, we found that not only ZO-1 but also β-catenin translocates to the cell–cell contacts by overexpression of JAM-A, and found that a similar translocation is observed in cells treated with AAP (Fig. 1D). Furthermore, the invasion activity of MDA-MB-231 cells, judged by a transwell matrigel invasion assay, was significantly suppressed by treatment with AAP or over-expression of JAM-A (Fig. 1E). By use of HPLC analysis, we confirmed that 98.9 ± 3.74% of AAP in the medium was not metabolized or degraded after incubation for 4 days. Thus, the results in Fig. 1 strongly suggest that AAP induces differentiation of MDA-MB-231 cells. The results also suggest that overexpression of JAM-A in MDA-MB-231 cells also induces differentiation of MDA-MB-231 cells.

We then examined the effect of AAP on a differentiated breast cancer cell line, MCF-7 [10]. Without treatment with AAP, MCF-7 cells showed a cobble-stone-like structure and most of them were $CD44^{-/low}/CD24^{+}$ cells (Fig. 2A and B), as described previously [10]. Treatment with AAP did not affect these phenotypes (Fig. 2A and B). Furthermore, the treatment did not affect the mRNA expression of markers for differentiated and stem cells as distinctly (Fig. 2C) as

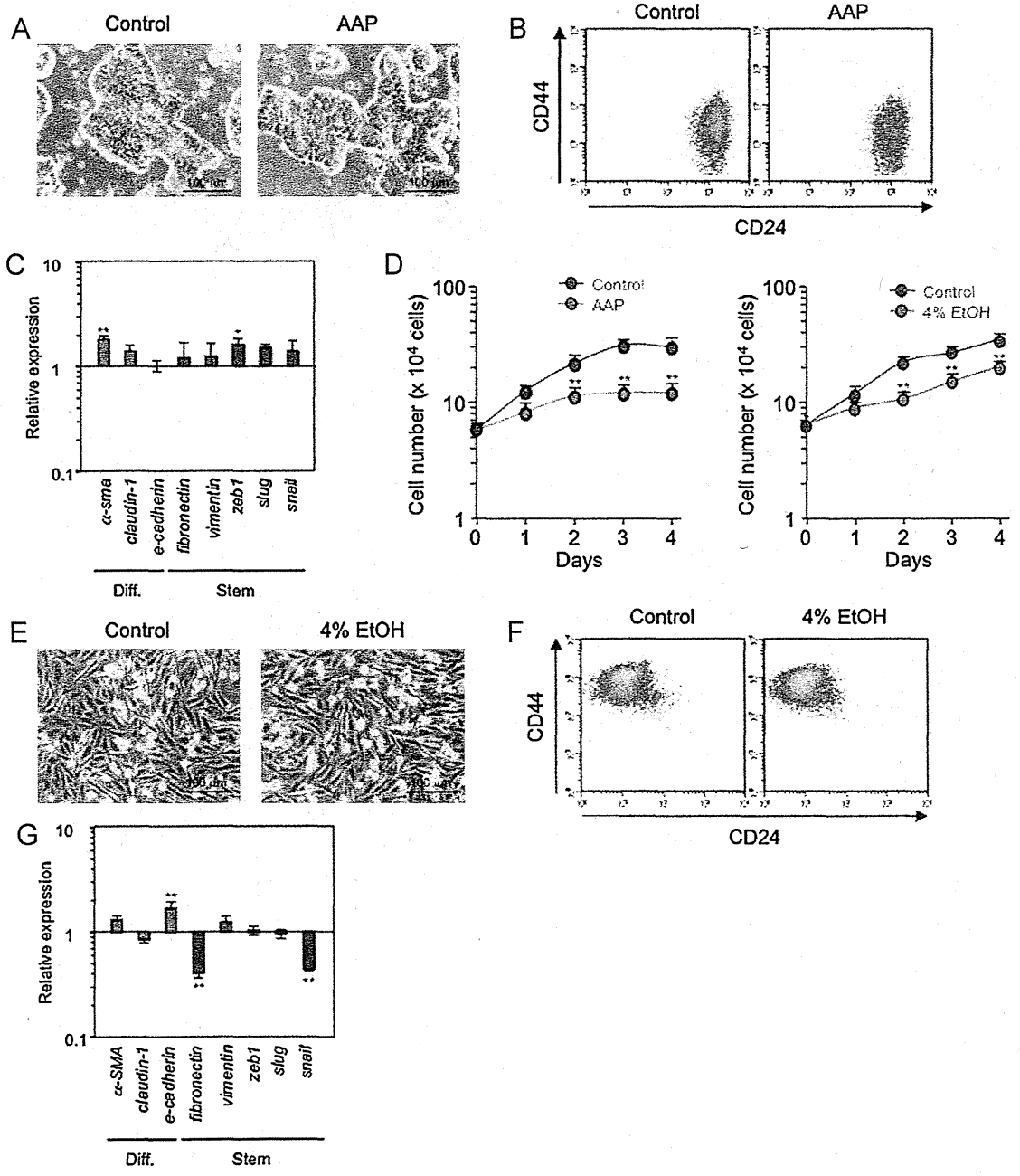

Fig. 2. Specificity of AAP-induced differentiation of MDA-MB-231 cells. MCF-7 (A–C) or MDA-MB-231 (D–G) cells were treated for 4 days with (AAP) or without (Control) 1 mM AAP (A–D) or 4% ethanol (EtOH) (D–G). Cell morphology (A and E), cell surface expression of CD24 and CD44 (B and F) and the mRNA expression (C and G) were examined as described in the legend of Fig. 1. The viable cell numbers were monitored by direct cell counting (D). Values shown are mean ± S.D. (n = 3–4). $^{*}P < 0.05$; $^{**}P < 0.01$.

was seen for MDA-MB-231 cells (Fig. 1C). These results suggest that AAP affects cell morphology, the expression of surface markers and the expression of differentiation-related genes specifically in undifferentiated (stem cell-like) breast cancer cells, supporting the notion that AAP induces differentiation of MDA-MB-231 cells.

Another characteristic feature of the induction of differentiation of CSCs is the inhibition of cell proliferation, and we showed that treatment with AAP suppressed the growth of MDA-MB-231 cells (Fig. 2D). Treatment of cells with 4% ethanol suppressed the growth of MDA-MB-231 cells similarly (Fig. 2D), however, this treatment did not affect cell morphology, the expression profile of CD44 and CD24, and mRNA expression of differentiation-related genes as distinctly (Fig. 2E–G) as that seen with AAP treatment (Fig. 1A–C). This finding suggests that AAP-dependent alterations of these phenotypes are not the result of cell growth inhibition.

3.2. Molecular mechanism for AAP-induced differentiation of MDA-MB-231 cells

In order to identify a structure–function relationship and molecular mechanism for AAP-induced differentiation of MDA-MB-231 cells, we examined the effects of various AAP derivatives (Fig. 3A) on the differentiation of MDA-MB-231 cells. As shown in Fig. 3B and C, of these AAP derivatives, compound e (*o*-acetamidophenol) increased the ratio of $CD44^{-/low}/CD24^{+}$ cells to total cells and induced the expression of claudin-1 to a similar extent as AAP, suggesting that *o*-acetamidophenol induces differentiation of MDA-MB-231 cells. Examination of the effect of each AAP derivative on cell growth revealed that not only AAP and *o*-acetamidophenol, but also some other derivatives (such as compound g) inhibit growth (Fig. 3D), confirming the idea that

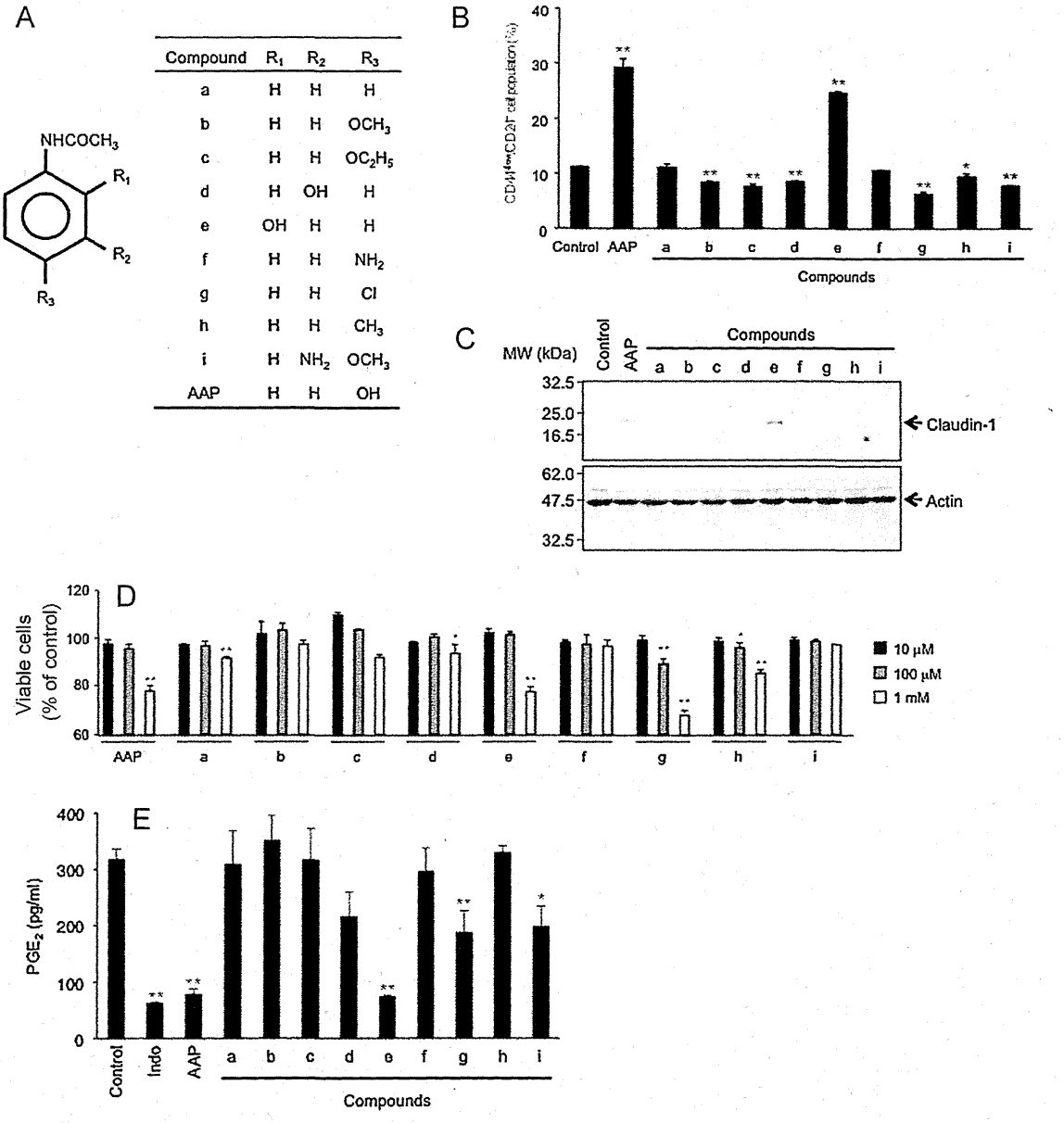

Fig. 3. Structure–function relationship of AAP for induction of differentiation of MDA-MB-231 cells. Chemical structures of AAP and its derivatives (compounds a–i) are shown (A). MDA-MB-231 cells were treated with or without (Control) 1 mM (B, C, E) or the indicated concentrations (D) of AAP and its derivatives or 0.1 mM indomethacin (Indo) (E) for 4 days (B–D) or 4 h (E). Cell surface expression of CD24 and CD44 was examined as described in the legend of Fig. 1 and the percentage of differentiated cells ($CD44^{-/low}/CD24^{+}$) to total cells was determined (B). Whole cell extracts were analyzed by immunoblotting with an antibody against claudin-1 or actin (C). The viable cell number was determined by the MTT method (D). Cells were further incubated with 50 μM arachidonic acid for 20 min and the amount of PGE_2 in the culture medium was determined by EIA (E). Values are mean ± S.D. ($n = 3$). $^{*}P < 0.05$; $^{**}P < 0.01$.

AAP-dependent alterations of differentiation-related phenotypes do not result from cell growth inhibition.

Using these AAP derivatives, we next examined the relationship between the anti-inflammatory activity and differentiation-inducing activity of AAP. The anti-inflammatory activity of each AAP derivative was estimated by its ability to decrease the level of PGE_2 in the culture medium. As shown in Fig. 3E, treatment of cells with 1 mM AAP decreased the PGE_2 level to a similar extent as 0.1 mM indomethacin. Furthermore, a similar decrease was observed with 1 mM *o*-acetamidophenol but not with other AAP derivatives (Fig. 3E), suggesting a close relationship between AAP's anti-inflammatory and differentiation-inducing activities.

As described in Section 1, various signaling pathways were reported to contribute to the maintenance of the stem cell-like properties of breast CSCs and mammary gland stem cells [24,25]. Therefore, we tried to identify the signaling pathway involved in maintaining the stem cell-like properties of MDA-MB-231 cells and AAP-dependent induction of differentiation. TGF-β1 is an important cytokine for maintenance of stem-cell like properties in various CSCs and normal stem cells and it has been reported that inhibition of the TGF-β signaling pathway induces differentiation of some CSCs [24]. Measurement of the expression of *tgf-β1* mRNA by real-time RT-PCR revealed that expression decreased after treatment of MDA-MB-231 cells with AAP (Fig. 4A). However, since an inhibitor of the TGF-β type I receptor (LY364947) did not affect the stem cell-like morphology of MDA-MB-231 cells (Fig. 4B), it is unlikely that the TGF-β signaling pathway contributes to the maintenance of stem

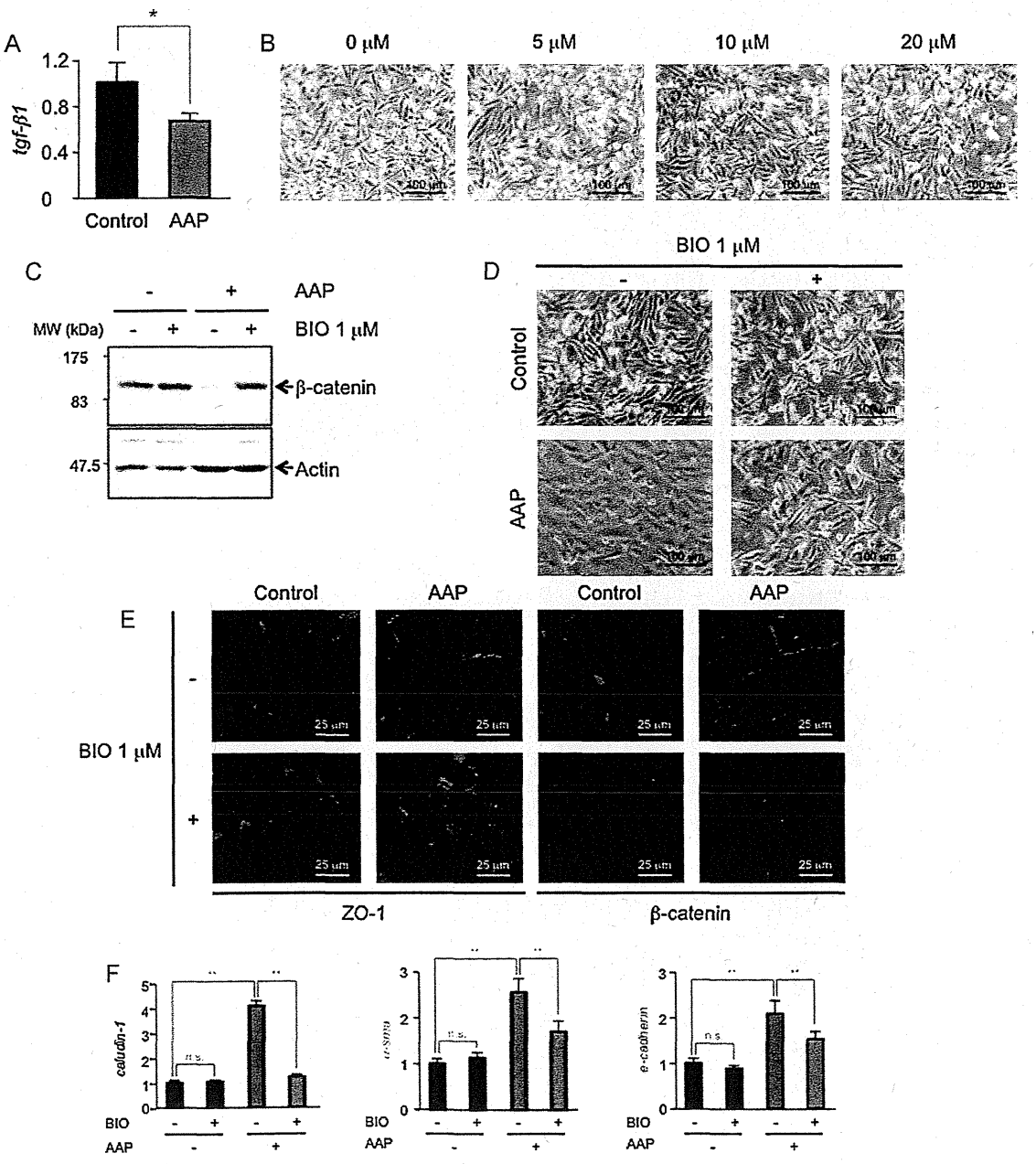

Fig. 4. Involvement of the Wnt/β-catenin canonical signaling pathway in AAP-induced differentiation of MDA-MB-231 cells. MDA-MB-231 cells were treated for 4 days with (AAP) or without (Control) 1 mM AAP in the presence or absence of 1 μM BIO (A, C–F). MDA-MB-231 cells were treated for 4 days with the indicated concentrations of LY364947 (B). The mRNA expression of each gene was examined and expressed as described in the legend of Fig. 1 (A and F). Cell morphology and expression of ZO-1 and β-catenin were examined as described in the legend of Fig. 1 (B, D, E). The amount of β-catenin was monitored by immunoblotting as described in the legend of Fig. 3 (C). Values shown are mean ± S.D. ($n = 3$–4). $^*P < 0.05$; $^{**}P < 0.01$; n.s., not significant.

cell-like properties and AAP-dependent induction of differentiation of MDA-MB-231 cells.

Next, we examined the contribution of the Wnt/β-catenin canonical signaling pathway. As shown in Fig. 4C, the level of β-catenin decreased clearly in cells treated with AAP and this decrease was suppressed by simultaneous treatment with BIO, a specific inhibitor of GSK3β [44], suggesting that the Wnt/β-catenin canonical signaling pathway is inhibited by the treatment with AAP. To examine the contribution of this inhibition to AAP-induced differentiation of MDA-MB-231 cells, we examined the effect of BIO on AAP-dependent alterations of phenotypes related to differentiation. Simultaneous treatment of cells with BIO suppressed AAP-dependent morphological change, translocation of ZO-1 and β-catenin to cell–cell contacts and up-regulation of mRNA expression of markers for differentiated cells (Fig. 4D–F). These results suggest that AAP induces differentiation of MDA-MB-231 cells through inhibition of the Wnt/β-catenin canonical signaling pathway.

3.3. An AAP-induced increase in susceptibility of MDA-MB-231 cells to anti-cancer drugs in vitro

High expression of ATP-binding cassette (ABC) transporters, such as multidrug resistance-associated proteins (MRPs) and multidrug resistance-1 (MDR1), which efflux intracellular anti-cancer drugs has been observed in various CSCs, and is responsible for their phenotypic resistance to chemotherapy [14,15,45]. Overexpression of MRPs (but not MDR1) in MDA-MB-231 cells and its contribution to multidrug resistance of the cells has been reported [46]. Therefore, the results described above suggest that treatment of MDA-MB-231 cells with AAP makes them more susceptible to anti-cancer drugs. In fact, pre-treatment of MDA-MB-231 cells with AAP made them more susceptible to doxorubicine or 5-fluorouracil (5-FU) (Fig. 5A). We also found that overexpression of JAM-A made MDA-MB-231 cells more susceptible to these anti-cancer drugs (Fig. 5B). On the other hand, pre-treatment of MCF-7 cells with AAP did not affect their sensitivity to these anti-cancer drugs (Fig. 5C), suggesting that AAP makes MDA-MB-231 cells more susceptible to anti-cancer drugs through induction of differentiation. We next examined the effect of treatment of MDA-MB-231 cells with AAP on the drug efflux activity by the calcein-AM accumulation assay. Due to its hydrophobicity calcein-AM is incorporated non-specifically into cells through cytoplasmic membranes and is then converted to a fluorescent molecule, calcein, in cells. Thus, an increase in the level of calcein in cells reflects a reduction in the drug efflux activity of cells [47]. As shown in Fig. 5D, a higher level of accumulation of

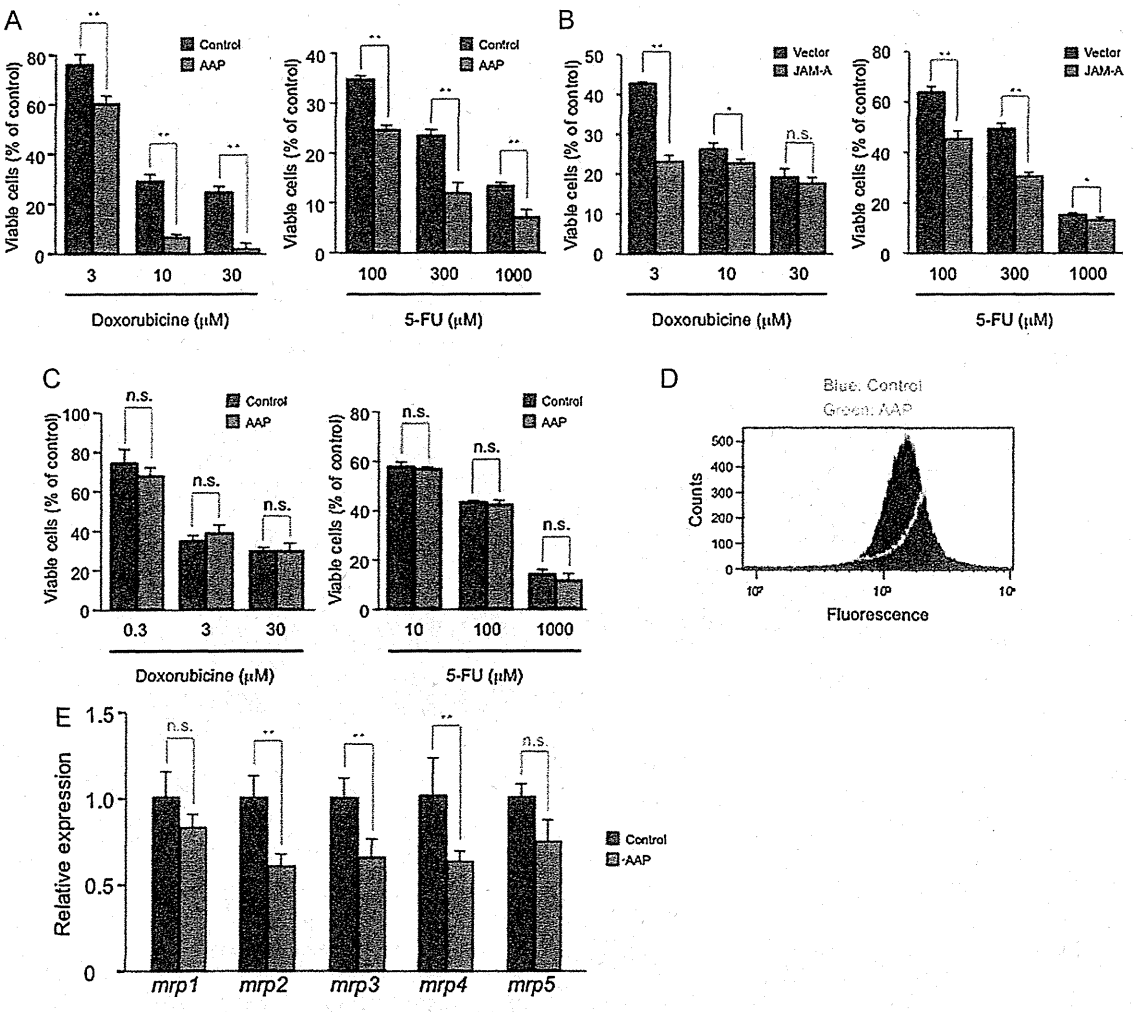

Fig. 5. AAP-induced increase in susceptibility of MDA-MB-231 cells to anti-cancer drugs. MDA-MB-231 (A, D, E) or MCF-7 (C) cells were treated with (AAP) or without (Control) 1 mM AAP for 4 days. MDA-MB-231 cells stably transfected with the expression plasmid for JAM-A (JAM-A) or vector (Vector) were cultured for 4 days (B). After collecting cells and re-plating in 24-well plates (6×10^4 cells for doxorubicine or 3×10^4 cells for 5-FU), cells were further incubated with the indicated concentrations of doxorubicine for 3 days or 5-FU for 5 days in the absence of AAP and cell viability was determined by MTT method (A–C). Cells were incubated with calcein-AM and the amounts of calcein in cells were monitored by FACS analysis as described in Section 2 (D). The mRNA expression of each gene was examined and expressed as described in the legend of Fig. 1 (E). Values shown are mean ± S.D. ($n = 3$–4). $^*P < 0.05$; $^{**}P < 0.01$; n.s., not significant.